Quantum Maxwell-Bloch equations for spatially inhomogeneous semiconductor lasers

Holger F. Hofmann and Ortwin Hess
Theoretical Quantum Electronics, Institute of Technical Physics, DLR Pfaffenwaldring 38-40, D-70569 Stuttgart, Germany
(Received 1 July 1998)

We present quantum Maxwell-Bloch equations (QMBE) for spatially inhomogeneous semiconductor laser devices. The QMBE are derived from fully quantum mechanical operator dynamics describing the interaction of the light field with the quantum states of the electrons and the holes near the band gap. By taking into account field-field correlations and field-dipole correlations, the QMBE include quantum noise effects, which cause spontaneous emission and amplified spontaneous emission. In particular, the source of spontaneous emission is obtained by factorizing the dipole-dipole correlations into a product of electron and hole densities. The QMBE are formulated for general devices, for edge emitting lasers and for vertical cavity surface emitting lasers, providing a starting point for the detailed analysis of spatial coherence in the near-field and far-field patterns of such laser diodes. Analytical expressions are given for the spectra of gain and spontaneous emission described by the QMBE. These results are applied to the case of a broad area laser, for which the frequency and carrier density dependent spontaneous emission factor β and the evolution of the far-field pattern near threshold are derived. [S1050-2947(99)02803-6]

PACS number(s): 42.55.Px, 42.50.Lc

I. INTRODUCTION

The spatiotemporal dynamics of semiconductor lasers can be simulated successfully by semiclassical Maxwell-Bloch equations without including any quantum effects in the light field (for an overview of the theory and modeling see [1] and references therein). The classical treatment of the light field is justified by the high intensity of the laser light well above threshold. However, the incoherent noise required by the uncertainty principle in both the electrical dipole of the semiconductor medium and the light field itself is of significant importance when several cavity modes compete or when the laser is close to threshold.

Photon rate equations for multimode operation of semiconductor lasers show that the spontaneous emission terms may contribute significantly to the spectral characteristics of the light field emitted by the laser [2,3]. Such models assume a fixed mode structure determined entirely by the empty cavity. This assumption does not apply to gain guided lasers and to unstable resonators, however [4–6]. In these cases it is therefore desirable to explicitly describe the spatial coherence of spontaneous emission.

The spatial coherence of spontaneous emission and amplified spontaneous emission is even more important in devices close to threshold or devices with a light field output dominated by spontaneous emission such as superluminescent diodes and ultralow threshold semiconductor lasers [7,8]. Ultralow threshold lasers may actually operate in a regime of negative gain where spontaneous emission is the only source of radiation [7]. A description of the light field emitted by such devices therefore requires an explicit description of the spatial coherence in spontaneous emission as well.

An approach to the consistent inclusion of the quantum noise properties of the light field in the dynamics of semiconductor laser diodes using nonequilibrium Green's functions has been presented in [9–11]. In this approach, the linear optical response of the medium is varied as a function of the time-dependent electron-hole distributions. Although the nonequilibrium Green's function presents an elegant solution for the description of many-body effects [9], the representation of the interband dipole dynamics by Green's functions causes a non-Markovian memory effect, which is difficult to handle and is therefore usually neglected [10]. Moreover, the need to determine the Green's function corresponding to the dynamically varying carrier distribution requires a computational effort far greater than that required for the integration of the corresponding Maxwell-Bloch equations. Therefore, as stated in [11], an exact analytical investigation of the spatial mode structures in realistic cavities using nonequilibrium Green's functions is out of reach. In order to simulate the spatiotemporal dynamics of multimode operation, of lasers near threshold, low threshold lasers or superluminescent diodes, it is therefore desireable to formulate an alternative approach to the problem of spontaneous emission and amplified spontaneous emission in such devices which is based on Maxwell-Bloch equations. By including the spatiotemporal dynamics of the interband dipole in such equations, non-Markovian terms are avoided and the quantum mechanical equations may be integrated in a straightforward manner.

The starting point for our description of quantum noise effects is the dynamics of quantum mechanical operators of the field and carrier system. Since the operator dynamics of the carrier system have been investigated in the context of Maxwell-Bloch equations before [12] and the light field equations correspond exactly to the classical Maxwell's equations, it is possible to focus only on the local light-matter interaction. Once the properties of this interaction are formulated in terms of the expectation values of field-field correlations, dipole-field correlations, carrier densities, fields, and dipoles, the dynamics of the carrier system and the light field propagation may be added.

In Sec. II, the quantum dynamics of the interaction between the light field and the carrier system is formulated in terms of Wigner distributions for the carriers and of spatially

continuous amplitudes for the light field. The equations are formulated for both bulk material and for quantum wells including the effects of anisotropic coupling to the polarization components of the light field. Section III summarizes the effects of the dynamics of the electron-hole system in the semiconductor material. The light field dynamics are introduced in Sec. IV. By quantizing Maxwell's equation, the coupling constant g_0 introduced in Sec. II is expressed in terms of the interband dipole matrix element. The complete set of quantum Maxwell-Bloch equations is presented in Sec. V. Based on this general formulation, specific approximate versions for quantum well edge emitting and vertical cavity surface emitting lasers are derived. The possibility of including two-time correlations in the quantum Maxwell-Bloch equations is discussed and equations are given for the case of vertical cavity surface emitting lasers. In Sec. VI, analytical results for the spectra of gain and spontaneous emission in quantum wells as well as the spontaneous emission factor β and the far-field pattern of amplified spontaneous emission in broad area quantum well lasers are presented. Section VII concludes the paper.

II. DYNAMICS OF THE LIGHT-CARRIER INTERACTION

A. Hamiltonian dynamics of densities and fields

In the following, we will describe the active semiconductor medium in terms of an isotropic two-band model where, for the case of the holes, a suitably averaged effective mass is taken [12]. A generalization to more bands is straightforward. In terms of the local annihilation operators for photons ($\hat{b}_{\mathbf{R}}$), electrons ($\hat{c}_{\mathbf{R}}$), and holes ($\hat{d}_{\mathbf{R}}$), the Hamiltonian of the light-carrier interaction can be written as

$$\hat{H}^{cL}=\hbar g_0 \sum_{\mathbf{R}} (\hat{b}^{\dagger}_{\mathbf{R}}\hat{c}_{\mathbf{R}}\hat{d}_{\mathbf{R}}+\hat{b}_{\mathbf{R}}\hat{c}^{\dagger}_{\mathbf{R}}\hat{d}^{\dagger}_{\mathbf{R}}). \tag{1}$$

The operator dynamics associated with this Hamiltonian are then given by

$$\left.\frac{\partial}{\partial t}\hat{b}_{\mathbf{R}}\right|_{cL} = -ig_0\hat{c}_{\mathbf{R}}\hat{d}_{\mathbf{R}}, \tag{2a}$$

$$\left.\frac{\partial}{\partial t}\hat{c}_{\mathbf{R}}\hat{d}_{\mathbf{R}'}\right|_{cL} = ig_0(\hat{b}_{\mathbf{R}}\hat{d}^{\dagger}_{\mathbf{R}}\hat{d}_{\mathbf{R}'}+\hat{b}_{\mathbf{R}'}\hat{c}^{\dagger}_{\mathbf{R}'}\hat{c}_{\mathbf{R}}-\hat{b}_{\mathbf{R}}\delta_{\mathbf{R},\mathbf{R}'}), \tag{2b}$$

$$\left.\frac{\partial}{\partial t}\hat{c}^{\dagger}_{\mathbf{R}}\hat{c}_{\mathbf{R}'}\right|_{cL} = -ig_0(\hat{b}_{\mathbf{R}'}\hat{c}^{\dagger}_{\mathbf{R}}\hat{d}^{\dagger}_{\mathbf{R}'}-\hat{b}^{\dagger}_{\mathbf{R}}\hat{c}_{\mathbf{R}'}\hat{d}_{\mathbf{R}}), \tag{2c}$$

$$\left.\frac{\partial}{\partial t}\hat{d}^{\dagger}_{\mathbf{R}}\hat{d}_{\mathbf{R}'}\right|_{cL} = -ig_0(\hat{b}_{\mathbf{R}'}\hat{c}^{\dagger}_{\mathbf{R}'}\hat{d}^{\dagger}_{\mathbf{R}}-\hat{b}^{\dagger}_{\mathbf{R}}\hat{c}_{\mathbf{R}}\hat{d}_{\mathbf{R}'}). \tag{2d}$$

The discrete positions $\mathbf{R}$ correspond to the lattice sites of the Bravais lattice describing the semiconductor crystal. Each lattice site actually represents the spatial volume ν_0 of the Wigner-Seitz cell of the lattice. For zinc-blende crystal structure, this volume is equal to one-quarter of the cubed lattice constant. In the case of $Al_{1-x}Ga_xAs$ structures the lattice constant is about 5.65×10^{-10} m and $\nu_0\approx4.5\times10^{-29}$ m^3 [13]. The photon annihilation operator $\hat{b}_{\mathbf{R}}$ therefore describes the annihilation of a photon within a volume ν_0. Here, we will focus on the light-carrier interaction and the quantum noise contributions responsible for spontaneous emission. For that purpose, we extend the semiclassical description by including not only the expectation values of the field and dipole operators, $\langle\hat{b}_{\mathbf{R}}\rangle$ and $\langle\hat{c}_{\mathbf{R}}\hat{d}_{\mathbf{R}'}\rangle$, respectively, but also the field-field correlations $\langle\hat{b}^{\dagger}_{\mathbf{R}}\hat{b}_{\mathbf{R}'}\rangle$ and the field-dipole correlation $\langle\hat{b}^{\dagger}_{\mathbf{R}}\hat{c}_{\mathbf{R}'}\hat{d}_{\mathbf{R}''}\rangle$. The factorized equations of motion then read

$$\left.\frac{\partial}{\partial t}\langle\hat{b}^{\dagger}_{\mathbf{R}}\hat{b}_{\mathbf{R}'}\rangle\right|_{cL} = -ig_0(\langle\hat{b}^{\dagger}_{\mathbf{R}}\hat{c}_{\mathbf{R}'}\hat{d}_{\mathbf{R}'}\rangle-\langle\hat{b}^{\dagger}_{\mathbf{R}'}\hat{c}_{\mathbf{R}}\hat{d}_{\mathbf{R}}\rangle^*), \tag{3a}$$

$$\left.\frac{\partial}{\partial t}\langle\hat{b}^{\dagger}_{\mathbf{R}}\hat{c}_{\mathbf{R}'}\hat{d}_{\mathbf{R}''}\rangle\right|_{cL} = ig_0(\langle\hat{b}^{\dagger}_{\mathbf{R}}\hat{b}_{\mathbf{R}'}\rangle\langle\hat{d}^{\dagger}_{\mathbf{R}'}\hat{d}_{\mathbf{R}''}\rangle+\langle\hat{b}^{\dagger}_{\mathbf{R}}\hat{b}_{\mathbf{R}''}\rangle\langle\hat{c}^{\dagger}_{\mathbf{R}''}\hat{c}_{\mathbf{R}'}\rangle - \langle\hat{b}^{\dagger}_{\mathbf{R}}\hat{b}_{\mathbf{R}'}\rangle\delta_{\mathbf{R}',\mathbf{R}''})+ig_0\langle\hat{c}^{\dagger}_{\mathbf{R}}\hat{c}_{\mathbf{R}'}\rangle\langle\hat{d}^{\dagger}_{\mathbf{R}}\hat{d}_{\mathbf{R}''}\rangle, \tag{3b}$$

$$\left.\frac{\partial}{\partial t}\langle\hat{c}^{\dagger}_{\mathbf{R}}\hat{c}_{\mathbf{R}'}\rangle\right|_{cL} = ig_0(\langle\hat{b}^{\dagger}_{\mathbf{R}}\hat{c}_{\mathbf{R}'}\hat{d}_{\mathbf{R}}\rangle-\langle\hat{b}^{\dagger}_{\mathbf{R}'}\hat{c}_{\mathbf{R}}\hat{d}_{\mathbf{R}'}\rangle^*), \tag{3c}$$

$$\left.\frac{\partial}{\partial t}\langle\hat{d}^{\dagger}_{\mathbf{R}}\hat{d}_{\mathbf{R}'}\rangle\right|_{cL} = ig_0(\langle\hat{b}^{\dagger}_{\mathbf{R}}\hat{c}_{\mathbf{R}'}\hat{d}_{\mathbf{R}'}\rangle-\langle\hat{b}^{\dagger}_{\mathbf{R}'}\hat{c}_{\mathbf{R}'}\hat{d}_{\mathbf{R}}\rangle^*). \tag{3d}$$

Note that this set of equations already represents a closed description of the field dynamics. If, as in many experimental configurations, the absolute phase of the light field and dipole operators may be considered unknown, these equations are sufficient for a description of the light-carrier interaction. However, when two-time correlations are of interest or in the case of coherent excitation by injection of an external laser it may also be necessary to additionally consider the dynamics of the field and dipole expectation values, i.e.,

$$\left.\frac{\partial}{\partial t}\langle\hat{b}_{\mathbf{R}}\rangle\right|_{cL} = -ig_0\langle\hat{c}_{\mathbf{R}}\hat{d}_{\mathbf{R}}\rangle, \tag{3e}$$

$$\left.\frac{\partial}{\partial t}\langle\hat{c}_{\mathbf{R}}\hat{d}_{\mathbf{R}'}\rangle\right|_{cL} = ig_0(\langle\hat{b}_{\mathbf{R}}\rangle\langle\hat{d}^{\dagger}_{\mathbf{R}}\hat{d}_{\mathbf{R}'}\rangle + \langle\hat{b}_{\mathbf{R}'}\rangle\langle\hat{c}^{\dagger}_{\mathbf{R}'}\hat{c}_{\mathbf{R}}\rangle-\langle\hat{b}_{\mathbf{R}}\rangle\delta_{\mathbf{R},\mathbf{R}'}). \tag{3f}$$

B. Physical background of the factorization

In the following, we will briefly discuss the implications of the factorization performed in the derivation of Eq. (3a). In order to formulate the dynamics of the light-matter interaction without including higher-order correlations, three terms have been factorized in the time derivative of the field-dipole correlation (3b). The factorizations are

$$\langle\hat{b}^{\dagger}_{\mathbf{R}}\hat{b}_{\mathbf{R}''}\hat{c}^{\dagger}_{\mathbf{R}''}\hat{c}_{\mathbf{R}'}\rangle\approx\langle\hat{b}^{\dagger}_{\mathbf{R}}\hat{b}_{\mathbf{R}''}\rangle\langle\hat{c}^{\dagger}_{\mathbf{R}''}\hat{c}_{\mathbf{R}'}\rangle, \tag{4a}$$

$$\langle\hat{b}^{\dagger}_{\mathbf{R}}\hat{b}_{\mathbf{R}'}\hat{d}^{\dagger}_{\mathbf{R}'}\hat{d}_{\mathbf{R}''}\rangle\approx\langle\hat{b}^{\dagger}_{\mathbf{R}}\hat{b}_{\mathbf{R}'}\rangle\langle\hat{d}^{\dagger}_{\mathbf{R}'}\hat{d}_{\mathbf{R}''}\rangle, \tag{4b}$$

$$\langle \hat{c}^{\dagger}_{\mathbf{R}} \hat{c}_{\mathbf{R}'} \hat{d}^{\dagger}_{\mathbf{R}''} \hat{d}_{\mathbf{R}'''} \rangle \approx \langle \hat{c}^{\dagger}_{\mathbf{R}} \hat{c}_{\mathbf{R}'} \rangle \langle \hat{d}^{\dagger}_{\mathbf{R}''} \hat{d}_{\mathbf{R}'''} \rangle . \tag{4c}$$

No additional factorizations are necessary in the density dynamics of photons, electrons, and holes. The three factorizations are based on the assumption of statistical independence between the densities of photons, electrons and holes. Since we are not considering fluctuations in the particle densities, this is a necessary assumption.

Equations (4a) and (4b) separate the photon density from the carrier densities. These terms represent stimulated emission processes. Therefore, a correlation of the photon density with the carrier densities would lead to a modified stimulated emission rate. Below threshold, this effect will be small because the amplified spontaneous emission is distributed over many modes such that the local correlations between photon and carrier densities are weak. Above threshold, the photon number fluctuations in the lasing mode cause relaxation oscillations. The photon number fluctuations are nearly 90% out of phase with the carrier number fluctuations. Therefore, the time averaged correlation is still negligible.

Equation (4c) separates the electron and hole densities. This term represents the spontaneous emission caused by the simultaneous presence of electrons and holes in the same location. Although it is reasonable to assume that the high rate of scattering at high carrier densities effectively reduce all electron-hole correlations to zero, it is important to note that the interband dipole $\langle \hat{c}_{\mathbf{R}} \hat{d}_{\mathbf{R}'} \rangle$ implies a phase correlation between the electrons and the holes. In fact, the spontaneous emission term factorized according to Eq. (4c) originates from the dipole-dipole correlation $\langle \hat{c}^{\dagger}_{\mathbf{R}} \hat{d}^{\dagger}_{\mathbf{R}'} \hat{c}_{\mathbf{R}''} \hat{d}_{\mathbf{R}'''} \rangle$. Note that this term could also be factorized into the product of dipole operators $\langle \hat{c}_{\mathbf{R}} \hat{d}_{\mathbf{R}'} \rangle^{*} \langle \hat{c}_{\mathbf{R}''} \hat{d}_{\mathbf{R}'''} \rangle$. The dynamics of the field-field and the field-dipole correlations are then identical to the dynamics of the products of the fields and dipoles. Therefore, that factorization corresponds to the approximations of the conventional Maxwell-Bloch equations such as described in [12], which do not rigorously include spontaneous emission.

Generally, spontaneous emission must always arise from random phase fluctuations. These are given by the product of electron and hole densities. While the phase dependent dipole relaxes quickly due to scattering events, the carrier densities are preserved during scattering. Therefore

$$\langle \hat{c}_{\mathbf{R}} \hat{d}_{\mathbf{R}'} \rangle^{*} \langle \hat{c}_{\mathbf{R}''} \hat{d}_{\mathbf{R}'''} \rangle \ll \langle \hat{c}^{\dagger}_{\mathbf{R}} \hat{c}_{\mathbf{R}''} \rangle \langle \hat{d}^{\dagger}_{\mathbf{R}'} \hat{d}_{\mathbf{R}'''} \rangle \tag{5a}$$

is usually a good assumption in semiconductor systems. Note that this assumption does fail in the case of low carrier densities and high dipole inducing fields. However, this case only occurs if the light field is injected from an external source. In semiconductor lasers and in light emitting diodes, the major contribution to the dipole-dipole correlations stems from the product of electron and hole densities. To check the statistical independence of photon, electron, and hole densities, it is also convenient to check the corresponding inequality for the three particle coherence represented by the field-dipole correlation,

$$\langle \hat{b}^{\dagger}_{\mathbf{R}} \hat{c}_{\mathbf{R}'} \hat{d}_{\mathbf{R}''} \rangle^{*} \langle \hat{b}^{\dagger}_{R'''} \hat{c}_{\mathbf{R}''''} \hat{d}_{\mathbf{R}''''} \rangle \ll \langle \hat{b}^{\dagger}_{\mathbf{R}} \hat{b}_{\mathbf{R}'''} \rangle \langle \hat{c}^{\dagger}_{\mathbf{R}'} \hat{c}_{\mathbf{R}''''} \rangle \langle \hat{d}^{\dagger}_{\mathbf{R}''} \hat{d}_{\mathbf{R}''''} \rangle . \tag{5b}$$

Thus, if a calculation does not fulfill this requirement, particle density correlations additionally have to be taken into account.

C. Wigner function formulation

In order to connect the light-carrier interaction to the highly dissipative carrier transport equations, it is practical to transform the carrier and dipole densities using Wigner transformations [14]. Replacing the discrete density matrices by continuous ones obtained by polynomial interpolation will allow, e.g., for numerical purposes an arbitrary choice of the discretization scales, which generally will be much larger than a lattice constant. Analytically, it permits an application of differential operators. Physically, the particle densities are smooth functions over distances of several lattice constants. A coherence length shorter than, e.g., ten lattice constants would require $\mathbf{k}$ states with $|\mathbf{k}|$ of at least one 20th of the Brilloin zone diameter. In typical laser devices, however, the electrons and holes all accumulate near the fundamental gap at $\mathbf{k}=0$. Therefore, it is simply a matter of convenience to define the continuous densities such that

$$\rho^{e}(\mathbf{r}=\mathbf{R},\mathbf{r}'=\mathbf{R}') = \frac{1}{\nu_0} \langle \hat{c}^{\dagger}_{\mathbf{R}} \hat{c}_{\mathbf{R}'} \rangle , \tag{6a}$$

$$\rho^{h}(\mathbf{r}=\mathbf{R},\mathbf{r}'=\mathbf{R}') = \frac{1}{\nu_0} \langle \hat{d}^{\dagger}_{\mathbf{R}} \hat{d}_{\mathbf{R}'} \rangle , \tag{6b}$$

$$\rho^{dipole}(\mathbf{r}=\mathbf{R},\mathbf{r}'=\mathbf{R}') = \frac{1}{\nu_0} \langle \hat{c}_{\mathbf{R}} \hat{d}_{\mathbf{R}'} \rangle . \tag{6c}$$

These continuous functions may then be transformed into Wigner functions by

$$f^{e}(\mathbf{r},\mathbf{k}) = \int d^3\mathbf{r}' e^{-i\mathbf{k}\mathbf{r}'} \rho^{e}\left(\mathbf{r} - \frac{\mathbf{r}'}{2}, \mathbf{r} + \frac{\mathbf{r}'}{2} \right), \tag{7a}$$

$$f^{h}(\mathbf{r},\mathbf{k}) = \int d^3\mathbf{r}' e^{-i\mathbf{k}\mathbf{r}'} \rho^{h}\left(\mathbf{r} - \frac{\mathbf{r}'}{2}, \mathbf{r} + \frac{\mathbf{r}'}{2} \right), \tag{7b}$$

$$p(\mathbf{r},\mathbf{k}) = \int d^3\mathbf{r}' e^{-i\mathbf{k}\mathbf{r}'} \rho^{dipole}\left(\mathbf{r} - \frac{\mathbf{r}'}{2}, \mathbf{r} + \frac{\mathbf{r}'}{2} \right). \tag{7c}$$

The normalization of these Wigner functions has been chosen in such a way that a value of one represents the maximal phase space density possible for Fermions, that is, one particle per state. Since the density of states in the six-dimensional phase space given by $\mathbf{r}$ and $\mathbf{k}$ is $1/8\pi^3$, a factor of $1/8\pi^3$ will appear whenever actual carrier densities need to be obtained from the Wigner functions. However, the normalization in terms of the maximal possible phase space density is convenient because it represents the probability that a quantum state in a given region of phase space is occupied. Therefore, the Wigner distribution corresponding to the thermal equilibrium of a given particle density is directly given by the Fermi function.

To deal with the light field dynamics in the same manner, the field and field-field correlation variables must also be defined on a continuous length scale. In order to obtain photon densities, we define

$$\mathcal{E}(\mathbf{r}=\mathbf{R})=\frac{1}{\sqrt{\nu_0}}\langle\hat{b}_{\mathbf{R}}\rangle, \tag{8a}$$

$$I(\mathbf{r}=\mathbf{R};\mathbf{r}'=\mathbf{R}')=\frac{1}{\nu_0}\langle\hat{b}^{\dagger}_{\mathbf{R}}\hat{b}_{\mathbf{R}'}\rangle. \tag{8b}$$

Finally, the dipole-field correlation must be defined accordingly, such that

$$\Theta^{corr.}(\mathbf{r}=\mathbf{R};\mathbf{r}'=\mathbf{R}',\mathbf{r}''=\mathbf{R}'')=\frac{1}{\sqrt{\nu_0^3}}\langle\hat{b}^{\dagger}_{\mathbf{R}}\hat{c}_{\mathbf{R}'}\hat{d}_{\mathbf{R}''}\rangle, \tag{9}$$

$$C(\mathbf{r};\mathbf{r}',\mathbf{k})=\int d^3\mathbf{r}''e^{-i\mathbf{k}\mathbf{r}''}\Theta^{corr.}\left(\mathbf{r};\mathbf{r}'-\frac{\mathbf{r}''}{2},\mathbf{r}'+\frac{\mathbf{r}''}{2}\right). \tag{10}$$

With these new definitions, the light-carrier interaction dynamics can now be expressed in a form that considers both the position and the momentum of the electrons and holes. The dynamics of emission and absorption now reads

$$\left.\frac{\partial}{\partial t}I(\mathbf{r};\mathbf{r}')\right|_{cL}=-ig_0\frac{\sqrt{\nu_0}}{8\pi^3}\int d^3\mathbf{k}(C(\mathbf{r};\mathbf{r}',\mathbf{k})-C^*(\mathbf{r}';\mathbf{r},\mathbf{k})) \tag{11a}$$

$$\begin{aligned}\left.\frac{\partial}{\partial t}C(\mathbf{r};\mathbf{r}',\mathbf{k})\right|_{cL}&=ig_0\sqrt{\nu_0}\frac{1}{8\pi^3}\int d^3\mathbf{x}\int d^3\mathbf{q}e^{i\mathbf{q}\mathbf{x}}\\&\times\left[f^e\left(\mathbf{r}',\mathbf{k}+\frac{\mathbf{q}}{2}\right)\right.\\&\left.+f^h\left(\mathbf{r}',-\mathbf{k}+\frac{\mathbf{q}}{2}\right)-1\right]I(\mathbf{r};\mathbf{r}'+\mathbf{x})\\&+ig_0\sqrt{\nu_0}\frac{1}{8\pi^3}\int d^3\mathbf{q}e^{i\mathbf{q}(\mathbf{r}-\mathbf{r}')}\\&\times f^e\left(\frac{\mathbf{r}+\mathbf{r}'}{2},\mathbf{k}+\frac{\mathbf{q}}{2}\right)f^h\left(\frac{\mathbf{r}+\mathbf{r}'}{2},-\mathbf{k}+\frac{\mathbf{q}}{2}\right),\end{aligned} \tag{11b}$$

$$\begin{aligned}\left.\frac{\partial}{\partial t}f^e(\mathbf{r},\mathbf{k})\right|_{cL}&=ig_0\sqrt{\nu_0}\frac{1}{8\pi^3}\int d^3\mathbf{x}\int d^3\mathbf{q}e^{i\mathbf{q}\mathbf{x}}\\&\times\left[C\left(\mathbf{r}+\mathbf{x};\mathbf{r},\mathbf{k}+\frac{\mathbf{q}}{2}\right)-C^*\left(\mathbf{r}+\mathbf{x};\mathbf{r},\mathbf{k}+\frac{\mathbf{q}}{2}\right)\right],\end{aligned} \tag{11c}$$

$$\begin{aligned}\left.\frac{\partial}{\partial t}f^h(\mathbf{r},\mathbf{k})\right|_{cL}&=ig_0\sqrt{\nu_0}\frac{1}{8\pi^3}\int d^3\mathbf{x}\int d^3\mathbf{q}e^{i\mathbf{q}\mathbf{x}}\\&\times\left[C\left(\mathbf{r}+\mathbf{x};\mathbf{r},-\mathbf{k}+\frac{\mathbf{q}}{2}\right)\right.\\&\left.-C^*\left(\mathbf{r}+\mathbf{x};\mathbf{r},-\mathbf{k}+\frac{\mathbf{q}}{2}\right)\right],\end{aligned} \tag{11d}$$

$$\left.\frac{\partial}{\partial t}\mathcal{E}(\mathbf{r})\right|_{cL}=-ig_0\frac{\sqrt{\nu_0}}{8\pi^3}\int d^3\mathbf{k}p(\mathbf{r},\mathbf{k}), \tag{11e}$$

$$\begin{aligned}\left.\frac{\partial}{\partial t}p(\mathbf{r},\mathbf{k})\right|_{cL}&=ig_0\sqrt{\nu_0}\frac{1}{8\pi^3}\int d^3\mathbf{x}\int d^3\mathbf{q}e^{i\mathbf{q}\mathbf{x}}\left[f^e\left(\mathbf{r},\mathbf{k}+\frac{\mathbf{q}}{2}\right)\right.\\&\left.+f^h\left(\mathbf{r},-\mathbf{k}+\frac{\mathbf{q}}{2}\right)-1\right]\mathcal{E}(\mathbf{r}+\mathbf{x}).\end{aligned} \tag{11f}$$

D. Local approximation

The integrals over $\mathbf{x}$ and $\mathbf{q}$ represent seemingly nonlocal effects introduced by the transformation into Wigner functions. This property of the Wigner transformation retains the coherent effects in the carrier system. For the interaction of the carriers with the light field, it ensures momentum conservation by introducing a nonlocal phase correlation in the dipole field corresponding to the total momentum of the electron and hole concentrations involved. Effectively, the integral over $\mathbf{q}$ converts the momentum part of the Wigner distributions into a coherence length. This coherence length then reappears in the spatial structure of the dipole field and the electromagnetic field generated by the carrier distribution. However, the coherence length in the carrier system is usually much shorter than the optical wavelength. It can therefore be approximated by a spatial δ function. Here, we do this by noting that

$$\frac{1}{8\pi^3}\int d^3\mathbf{q}e^{i\mathbf{q}\mathbf{x}}=\delta(\mathbf{x}). \tag{12}$$

If the effects of the momentum shift $\mathbf{q}$ in the Wigner functions is neglected, the integrals may then be solved, yielding only local interactions between the carrier system and the light field:

$$\left.\frac{\partial}{\partial t}I(\mathbf{r};\mathbf{r}')\right|_{cL}=-ig_0\frac{\sqrt{\nu_0}}{8\pi^3}\int d^3\mathbf{k}(C(\mathbf{r};\mathbf{r}',\mathbf{k})-C^*(\mathbf{r}';\mathbf{r},\mathbf{k})), \tag{13a}$$

$$\begin{aligned}\left.\frac{\partial}{\partial t}C(\mathbf{r};\mathbf{r}',\mathbf{k})\right|_{cL}&=ig_0\sqrt{\nu_0}[f^e(\mathbf{r}',\mathbf{k})+f^h(\mathbf{r}',-\mathbf{k})-1]I(\mathbf{r};\mathbf{r}')\\&+ig_0\sqrt{\nu_0}\delta(\mathbf{r}-\mathbf{r}')f^e(\mathbf{r},\mathbf{k})f^h(\mathbf{r},-\mathbf{k}),\end{aligned} \tag{13b}$$

$$\left.\frac{\partial}{\partial t}f^e(\mathbf{r},\mathbf{k})\right|_{cL}=ig_0\sqrt{\nu_0}(C(\mathbf{r};\mathbf{r},\mathbf{k})-C^*(\mathbf{r};\mathbf{r},\mathbf{k})) \tag{13c}$$

$$\left.\frac{\partial}{\partial t}f^h(\mathbf{r},\mathbf{k})\right|_{cL}=ig_0\sqrt{\nu_0}(C(\mathbf{r};\mathbf{r},-\mathbf{k})-C^*(\mathbf{r};\mathbf{r},-\mathbf{k})), \tag{13d}$$

$$\left.\frac{\partial}{\partial t}\mathcal{E}(\mathbf{r})\right|_{cL}=-ig_0\frac{\sqrt{\nu_0}}{8\pi^3}\int d^3\mathbf{k}p(\mathbf{r},\mathbf{k}) \tag{13e}$$

$$\left.\frac{\partial}{\partial t}p(\mathbf{r},\mathbf{k})\right|_{cL} = ig_0\sqrt{\nu_0}(f^e(\mathbf{r},\mathbf{k}) + f^h(\mathbf{r},-\mathbf{k}) - 1)\mathcal{E}(\mathbf{r}). \tag{13f}$$

These equations now provide a compact description of the light-carrier interaction in a three-dimensional semiconductor medium, including the incoherent quantum noise term, which is the source of spontaneous emission.

E. Light-carrier interaction for quantum wells

Similar equations may also be formulated for a quantum well structure by replacing the phase space density of $1/8\pi^3$ with $1/4\pi^2$, reducing the spatial coordinates of the carrier system to two dimensions, and introducing a δ function for the coordinate perpendicular to the quantum well at the points where field coordinates correspond to dipole coordinates. Of course, the electromagnetic field remains three-dimensional, even though the dipole it originates from is confined to two dimensions. In particular, the correlation $C(\mathbf{r};\mathbf{r}',\mathbf{k})$ has both a three dimensional coordinate $\mathbf{r}$ and a two-dimensional coordinate $\mathbf{r}'$. It is therefore useful to distinguish the two-dimensional and the three-dimensional coordinates. In the following, the two-dimensional carrier coordinates will be marked with the index $\|$. Note that, in some cases, both $\mathbf{r}$ and $\mathbf{r}_\|$ appear in the equations. In those cases, the in-plane coordinates r_x and r_y are equal, while the perpendicular coordinate r_z must be equal to the quantum well coordinate z_0. The equations for the interaction of the three-dimensional light field with the two-dimensional electron-hole system in a single quantum well subband then read

$$\left.\frac{\partial}{\partial t}I(\mathbf{r};\mathbf{r}')\right|_{cL} = -ig_0\frac{\sqrt{\nu_0}}{4\pi^2}\int d^2\mathbf{k}_\|(C(\mathbf{r};\mathbf{r}'_\|,\mathbf{k}_\|)\,\delta(r'_z - z_0) - C^*(\mathbf{r}';\mathbf{r}_\|,\mathbf{k}_\|)\,\delta(r_z - z_0)), \tag{14a}$$

$$\left.\frac{\partial}{\partial t}C(\mathbf{r};\mathbf{r}'_\|,\mathbf{k}_\|)\right|_{cL} = ig_0\sqrt{\nu_0}(f^e(\mathbf{r}'_\|,\mathbf{k}_\|) + f^h(\mathbf{r}'_\|,-\mathbf{k}_\|) - 1)I(\mathbf{r};\mathbf{r}')_{r'_z=z_0} + ig_0\sqrt{\nu_0}\delta(\mathbf{r}_\| - \mathbf{r}'_\|)\,\delta(r_z - z_0) \times f^e(\mathbf{r}_\|,\mathbf{k}_\|)f^h(\mathbf{r}_\|,-\mathbf{k}_\|), \tag{14b}$$

$$\left.\frac{\partial}{\partial t}f^e(\mathbf{r}_\|,\mathbf{k}_\|)\right|_{cL} = ig_0\sqrt{\nu_0}(C(\mathbf{r};\mathbf{r}_\|,\mathbf{k}_\|)_{r_z=z_0} - C^*(\mathbf{r};\mathbf{r}_\|,\mathbf{k}_\|)_{r_z=z_0}), \tag{14c}$$

$$\left.\frac{\partial}{\partial t}f^h(\mathbf{r}_\|,\mathbf{k}_\|)\right|_{cL} = ig_0\sqrt{\nu_0}(C(\mathbf{r};\mathbf{r}_\|,-\mathbf{k}_\|)_{r_z=z_0} - C^*(\mathbf{r};\mathbf{r}_\|,-\mathbf{k}_\|)_{r_z=z_0}), \tag{14d}$$

$$\left.\frac{\partial}{\partial t}\mathcal{E}(\mathbf{r})\right|_{cL} = -ig_0\frac{\sqrt{\nu_0}}{4\pi^2}\int d^2\mathbf{k}_\| p(\mathbf{r}_\|,\mathbf{k}_\|)\,\delta(r_z - z_0), \tag{14e}$$

$$\left.\frac{\partial}{\partial t}p(\mathbf{r}_\|,\mathbf{k}_\|)\right|_{cL} = ig_0\sqrt{\nu_0}(f^e(\mathbf{r}_\|,\mathbf{k}_\|) + f^h(\mathbf{r}_\|,-\mathbf{k}_\|) - 1)\mathcal{E}(\mathbf{r})_{r_z=z_0}. \tag{14f}$$

Note that the value of g_0 will usually be slightly lower than the bulk value because the overlap of the spatial wave functions of the electrons and the holes in the lowest subbands is less than one. The equations derived above represent the interaction of a single conduction band and a single valence band with a single scalar light field. Neither the spin degeneracy of the carriers nor the polarization of the light field has been considered.

F. Spin degeneracy and light field polarization

Since the geometry of light field emission is highly dependent on polarization effects such effects should also be taken into account in the framework of this theory. The basic interaction between a single conduction band, a single valence band and a single light field polarization are accurately represented by Eqs. (13a–13f) and (14a–14f). By adding the contributions of separate transitions, any many band system may be described based on these equations. In semiconductor quantum wells the situation is considerably simplified if only the lowest subbands are considered. Then there are only two completely separate transitions involving circular light field polarizations coupled to a single one of the two electron and hole bands. The quantum well structure does not interact with light fields that are linearly polarized in the direction perpendicular to the plane of the quantum well. The equations for quantum wells are therefore completed by adding an index of $+$ or $-$ to each variable.

The situation in the bulk system is much more involved. The transitions occur between the twofold degenerate spin 1/2 system of the electrons and the fourfold degenerate spin 3/2 system of the holes. All three polarization directions of the light field are equally possible, connecting each of the electron bands with three of the four hole bands. However, since the effective mass of the two heavy-hole bands is much larger than the effective mass of the light holes (e.g. by a factor of 8 in GaAs), only a small fraction of the holes will be in the light-hole bands (about 6% in GaAs for equilibrium distributions). Consequently, the carrier subsystem can again be separated into two pairs of bands. However, the light field polarization emitted by the electron-heavy hole transitions in bulk material is circularly polarized with respect to the relative momentum $2\mathbf{k}$ of the electron and the heavy hole. Since usually there is no strong directional anisotropy in the $\mathbf{k}$ space distribution of the carriers, it can be assumed that one third of the $\mathbf{k}$ space volume contributes to each polarization direction and the equations may be formulated accordingly.

In the following, we will assume that the Wigner distributions of the two pairs of bands considered are approximately equal at all times. Note that this means that hole burning effects in the spin and polarization dynamics that may occur in vertical cavity surface emitting lasers [15] are ignored. However, such effects have been investigated in several other studies [16–19] and are found to be fairly weak in some devices [20].

The complete set of dynamical equations can now be formulated by adding the carrier dynamics and the linear part of Maxwell's equations to the light-carrier interaction.

III. CARRIER DYNAMICS

Modeling the carrier dynamics of a semiconductor system can be a formidable task all by itself. A number of approximations and models have been developed to deal with the effects of many-particle interactions and correlations and with the dissipation caused by the electron-phonon interactions [21,22]. In the following, we choose a simple diffusion model. Many-particle effects such as the band-gap renormalization or the Coulomb enhancement are not mentioned explicitly, but can be added in a straightforward manner [1,12].

We assume that the electron and hole densities will be kept equal by the Coulomb interaction, which will induce a current whenever charges are separated. Therefore, it is possible to define the ambipolar carrier density $N(\mathbf{r})$ with

$$N(\mathbf{r})=\frac{1}{4\pi^3}\int d^3\mathbf{k} f^e(\mathbf{r},\mathbf{k})=\frac{1}{4\pi^3}\int d^3\mathbf{k} f^h(\mathbf{r},\mathbf{k}). \quad (15)$$

Note that the twofold degeneracy of the electron and heavy-hole bands has been included by choosing a density of states of $1/4\pi^3$ instead of $1/8\pi^3$. This includes the assumption that the Wigner distribution does not depend on the spin variable of the electrons and holes as mentioned above.

The light carrier interaction of this carrier density is

$$\left.\frac{\partial}{\partial t}N(\mathbf{r})\right|_{cL}=ig_0\frac{\sqrt{\nu_0}}{4\pi^3}\int d^3\mathbf{k}\sum_i [C_{ii}(\mathbf{r};\mathbf{r},\mathbf{k})-C_{ii}^*(\mathbf{r};\mathbf{r},\mathbf{k})]$$
$$=-\frac{\partial}{\partial t}\sum_i I_{ii}(\mathbf{r};\mathbf{r})_{cL}, \quad (16)$$

where the index i denotes the component of the light field or dipole density corresponding to the linear polarization direction of $i=x,y,z$. In the case of $C_{ij}(\mathbf{r};\mathbf{r}',\mathbf{k})$ the index i refers to the field polarization and the second index j denotes the vector component of the dipole vector. Equation (16) shows how the field-dipole correlation converts electron-hole pairs into photons. The total carrier density dynamics can now be formulated as

$$\frac{\partial}{\partial t}N(\mathbf{r})=D_{amb}\Delta N(\mathbf{r})+j(\mathbf{r})-\gamma N(\mathbf{r})+ig_0\frac{\sqrt{\nu_0}}{4\pi^3}$$
$$\times\int d^3\mathbf{k}\sum_i [C_{ii}(\mathbf{r};\mathbf{r},\mathbf{k})-C_{ii}^*(\mathbf{r};\mathbf{r},\mathbf{k})], \quad (17)$$

where D_{amb} is the ambipolar diffusion constant, $j(\mathbf{r})$ is the injection current density, and γ is the rate of spontaneous recombinations by nonradiative processes and/or spontaneous emission into modes not considered in $I_{ij}(\mathbf{r},\mathbf{r}')$, e.g., if the paraxial approximation is applied.

The $\mathbf{k}$ dependence of the distribution functions $f^e(\mathbf{r},\mathbf{k})$ and $f^h(\mathbf{r},\mathbf{k})$ may be approximated by assuming that the electrons and holes will always be in thermal equilibrium. The distribution functions are then given by Fermi functions

$$f_{eq}^{e,h}(\mathbf{r},\mathbf{k})=\left(\exp\left[\frac{1}{k_BT}\left(\frac{\hbar^2\mathbf{k}^2}{2m_{eff}^{e,h}}-\mu^{e,h}(\mathbf{r})\right)\right]+1\right)^{-1}, \quad (18)$$

where $m_{eff}^{e,h}$ are the effective masses of electrons and heavy holes, respectively. The chemical potential $\mu^{e,h}(\mathbf{r})$ is a function of the carrier density $N(\mathbf{r})$. A useful estimate of this relationship is given by the Pade approximation [12,23]. Spectral hole burning may be taken into account by introducing a relaxation time τ_r and converting the dynamics of the distribution function due to the light-carrier interaction into a deviation from the equilibrium distribution by adiabatic elimination of the relaxation dynamics:

$$f^{e,h}(\mathbf{r},\mathbf{k})=f_{eq}^{e,h}(\mathbf{r},\mathbf{k})+ig_0\sqrt{\nu_0}\tau_r$$
$$\times\sum_i [C_{ii}(\mathbf{r};\mathbf{r},\pm\mathbf{k})-C_{ii}^*(\mathbf{r};\mathbf{r},\pm\mathbf{k})]. \quad (19)$$

Finally, the carrier dynamics of the dipole $p(\mathbf{r},\mathbf{k})$ and the dipole part of the field-dipole correlation $C(\mathbf{r};\mathbf{r}',\mathbf{k})$ needs to be formulated. Since both depend on a correlation of the electrons with the holes, they will necessarily relax rather quickly at a rate of $\Gamma(\mathbf{k})$, which should be of the same order of magnitude as $1/\tau_r$. Physically, $\Gamma(\mathbf{k})$ may be interpreted as the total momentum dependent scattering rate in the carrier system. The remainder of the dynamics can be derived from the single-particle dynamics. This unitary contribution to the evolution of the dipole may be expressed by a momentum dependent frequency $\Omega(\mathbf{k})$. For parabolic bands and isotropic effective masses $m_{eff}^{e/h}$, this frequency is given by

$$\Omega(\mathbf{k})=\left(\frac{\hbar}{2m_{eff}^e}+\frac{\hbar}{2m_{eff}^h}\right)\mathbf{k}^2. \quad (20)$$

Many-particle effects due to the Coulomb interaction between the carriers may be included by introducing a carrier density dependence in $\Gamma[\mathbf{k},N(\mathbf{r})]$ and $\Omega[\mathbf{k},N(\mathbf{r})]$. Such renormalization terms representing the mean field effects of the carrier-carrier interaction have been derived and discussed, e.g., in [12]. In the following, this many-particle renormalization will not be mentioned explicitly, although it can be included in a straightforward manner.

With the rates $\Gamma(\mathbf{k})$ and $\Omega(\mathbf{k})$ the dipole dynamics reads

$$\left.\frac{\partial}{\partial t}C_{ij}(\mathbf{r};\mathbf{r}',\mathbf{k})\right|_c=-[\Gamma(\mathbf{k})+i\Omega(\mathbf{k})]C_{ij}(\mathbf{r};\mathbf{r}',\mathbf{k}), \quad (21a)$$

$$\left.\frac{\partial}{\partial t}p_i(\mathbf{r},\mathbf{k})\right|_c=-[\Gamma(\mathbf{k})+i\Omega(\mathbf{k})]p_i(\mathbf{r},\mathbf{k}). \quad (21b)$$

Note that the phase dynamics is formulated relative to the band-gap frequency ω_0. The real physical phase oscillations of $p(\mathbf{r},\mathbf{k})$ would include an additional phase factor of $\exp[-i\omega_0 t]$. However, the only physical effect of this oscillation is to establish resonance with the corresponding frequency range in the electromagnetic field, the dynamics of which we consider next.

IV. MAXWELL'S EQUATION

The Heisenberg equations of motion describing the operator dynamics of the electromagnetic field operators are identical to the classical Maxwell's equations. In terms of the electromagnetic field $\mathbf{E}(\mathbf{r})$ and the dipole densities $\mathbf{P}(\mathbf{r})$, the equation reads

$$\boldsymbol{\nabla}\times[\boldsymbol{\nabla}\times\mathbf{E}(\mathbf{r})]+\frac{\epsilon_r}{c^2}\frac{\partial^2}{\partial t^2}\left(\mathbf{E}(\mathbf{r})+\frac{1}{\epsilon_r\epsilon_0}\mathbf{P}(\mathbf{r})\right)=0, \quad (22)$$

where ϵ_0 and c are the dielectric constant and the speed of light in vacuum, respectively, and $\epsilon_r\epsilon_0$ is the dielectric constant in the background semiconductor medium.

Maxwell's equation describes the light field dynamics for all frequencies. Since we are only interested in frequencies near the band-gap frequency ω_0, it is useful to separate the phase factor of $\exp[-i\omega_0 t]$, defining $\mathbf{E}(\mathbf{r})=\exp[-i\omega_0 t]\mathbf{E_0}(\mathbf{r})$. Now $\mathbf{E}_0(\mathbf{r})$ can be considered to vary slowly in time relative to $\exp[-i\omega_0 t]$. Therefore, the time derivatives may be approximated by

$$\exp[i\omega_0 t]\frac{\partial^2}{\partial t^2}\exp[-i\omega_0 t]\mathbf{E}_0(\mathbf{r})$$

$$\approx-\omega_0^2\mathbf{E}_0(\mathbf{r})-2i\omega_0\frac{\partial}{\partial t}\mathbf{E}_0(\mathbf{r}). \quad (23)$$

Similarly, $\mathbf{P}_0(\mathbf{r})$ may be defined such that $\mathbf{P}(\mathbf{r})=\exp[-i\omega_0 t]\mathbf{P}_0(\mathbf{r})$. The approximation used here may even be of zero order, since we are primarily interested in the dynamics of the electromagnetic field:

$$\exp[i\omega_0 t]\frac{\partial^2}{\partial t^2}\exp[-i\omega_0 t]\mathbf{P}_0(\mathbf{r})\approx-\omega_0^2\mathbf{P}_0(\mathbf{r}). \quad (24)$$

The temporal evolution of the electromagnetic field now reads

$$\frac{\partial}{\partial t}\mathbf{E}_0(\mathbf{r})=-i\frac{\omega_0}{2k_0^2\epsilon_r}\{\boldsymbol{\nabla}\times[\boldsymbol{\nabla}\times\mathbf{E}_0(\mathbf{r})]$$

$$-\epsilon_r k_0^2\mathbf{E}_0(\mathbf{r})\}-i\frac{\omega_0}{2\epsilon_r\epsilon_0}\mathbf{P}_0(\mathbf{r}), \quad (25)$$

where $k_0=\omega_0/c$ is the vacuum wave-vector length corresponding to ω_0. In Eq. (25), the field dynamics is described in terms of electromagnetic units, that is the fields represent forces acting on charges. To switch scales to the photon densities represented by $\mathcal{E}(\mathbf{r})$, energy densities have to be considered. Since the energy of each photon will be close to the band-gap energy $\hbar\omega_0$, the energy density of the electromagnetic field is given by

$$\hbar\omega_0\mathcal{E}^*(\mathbf{r})\mathcal{E}(\mathbf{r})=\frac{\epsilon_r\epsilon_0}{2}\mathbf{E}_0^*(\mathbf{r})\mathbf{E}_0^*(\mathbf{r}). \quad (26)$$

Therefore, the field may be expressed as photon density amplitude using

$$\mathbf{E}_0(\mathbf{r})=\sqrt{\frac{2\hbar\omega_0}{\epsilon_r\epsilon_0}}\mathcal{E}(\mathbf{r}). \quad (27)$$

The dipole density $\mathbf{P}_0(\mathbf{r})$ may be expressed in terms of $\rho^{dipole}(\mathbf{r},\mathbf{r})$ and $\mathbf{p}(\mathbf{r},\mathbf{k})$ by noting that the density $\rho^{dipole}(\mathbf{r},\mathbf{r})$ is the dipole density in units of one-half the atomic dipole given by the interband dipole matrix element $\mathbf{d}_{cv}$ at $k=0$. The factor of one-half is a logical consequence of the property that $\langle\hat{c}_{\mathbf{R}}\hat{d}_{\mathbf{R}'}\rangle\leqslant 1/2$. Thus, a fully polarized lattice would have a dipole density of $\rho^{dipole}(\mathbf{r},\mathbf{r}=1)/(2\nu_0)$, which must correspond to $\mathbf{P}(\mathbf{r})=\mathbf{d}_{cv}/\nu_0$. Note that $\mathbf{d}_{cv}$ contains an arbitrary phase factor depending only on the definition of the states used for its determination. For convenience, we assume a definition of phases such that $\mathbf{d}_{cv}$ is real. The dipole density $\mathbf{P}_0(\mathbf{r})$ may then be written as

$$\mathbf{P}(\mathbf{r})=2\mathbf{d}_{cv}\rho^{dipole}=\frac{2|\mathbf{d_{cv}}|}{8\pi^3}\int d^3\mathbf{k}\mathbf{p}(\mathbf{r},\mathbf{k}). \quad (28)$$

Written in terms of $\mathcal{E}(\mathbf{r})$ and $\mathbf{p}(\mathbf{r},\mathbf{k})$, the complete field dynamics now reads

$$\frac{\partial}{\partial t}\mathcal{E}(\mathbf{r})=-i\frac{\omega_0}{2k_0^2\epsilon_r}\{\nabla\times[\nabla\times\mathcal{E}(\mathbf{r})]-\epsilon_r k_0^2\mathcal{E}(\mathbf{r})\}$$

$$-i\sqrt{\frac{\omega_0}{2\hbar\epsilon_r\epsilon_0}}\frac{|\mathbf{d_{cv}}|}{8\pi^3}\int d^3\mathbf{k}\mathbf{p}(\mathbf{r},\mathbf{k})$$

$$=-i\frac{\omega_0}{2k_0^2\epsilon_r}\{\nabla\times[\nabla\times\mathcal{E}(\mathbf{r})]-\epsilon_r k_0^2\mathcal{E}(\mathbf{r})\}$$

$$-ig_0\frac{\sqrt{\nu_0}}{8\pi^3}\int d^3\mathbf{k}\mathbf{p}(\mathbf{r},\mathbf{k}). \quad (29)$$

The coupling frequency g_0 introduced in Eq. (1) may be expressed in terms of the dipole matrix element $\mathbf{d_{cv}}$:

$$g_0=\sqrt{\frac{\omega_0}{2\hbar\epsilon_r\epsilon_0\nu_0}}|\mathbf{d_{cv}}|. \quad (30)$$

With this equation, the operator dynamics of the light field operator $\hat{b}_{\mathbf{R}}$ corresponds to the field dynamics of the Maxwell-Bloch equations for classical fields. By applying the linear propagation dynamics of the field to $I_{ij}(\mathbf{r};\mathbf{r}')$ and $C_{ij}(\mathbf{r};\mathbf{r}',\mathbf{k})$ as well, it is now possible to formulate a complete set of quantum Maxwell-Bloch equations.

V. QUANTUM MAXWELL-BLOCH EQUATIONS

A. Quantum Maxwell-Bloch equations for a three-dimensional gain medium

On the basis of the discussion in the previous sections, the quantum Maxwell-Bloch equations for a bulk gain medium in three dimensions read

$$\frac{\partial}{\partial t}N(\mathbf{r})=D_{amb}\Delta N(\mathbf{r})+j(\mathbf{r})-\gamma N(\mathbf{r})+ig_0\frac{\sqrt{\nu_0}}{8\pi^3}\int d^3\mathbf{k}\sum_i\,[C_{ii}(\mathbf{r};\mathbf{r},\mathbf{k})-C_{ii}^*(\mathbf{r};\mathbf{r},\mathbf{k})], \tag{31a}$$

$$\begin{aligned}\frac{\partial}{\partial t}C_{ij}(\mathbf{r};\mathbf{r}',\mathbf{k})&=-[\Gamma(\mathbf{k})+i\Omega(\mathbf{k})]C_{ij}(\mathbf{r};\mathbf{r}',\mathbf{k})\\&\quad-i\frac{\omega_0}{2k_0^2}\Bigg(\sum_k\frac{\partial}{\partial r_k}\epsilon_r^{-1}\frac{\partial}{\partial r_k}C_{ij}(\mathbf{r};\mathbf{r}',\mathbf{k})\\&\quad-\sum_k\frac{\partial}{\partial r_i}\epsilon_r^{-1}\frac{\partial}{\partial r_k}C_{kj}(\mathbf{r};\mathbf{r}',\mathbf{k})+k_0^2C_{ij}(\mathbf{r};\mathbf{r}',\mathbf{k})\Bigg)\\&\quad+ig_0\frac{2\sqrt{\nu_0}}{3}[f_{eq}^e(k;N(\mathbf{r}'))\\&\quad+f_{eq}^h(k;N(\mathbf{r}'))-1]I_{ij}(\mathbf{r};\mathbf{r}')\\&\quad+ig_0\frac{2\sqrt{\nu_0}}{3}\delta(\mathbf{r}-\mathbf{r}')\,\delta_{ij}f_{eq}^e(k;N(\mathbf{r}))f_{eq}^h(k;N(\mathbf{r})),\end{aligned} \tag{31b}$$

$$\begin{aligned}\frac{\partial}{\partial t}I_{ij}(\mathbf{r};\mathbf{r}')&=-i\frac{\omega_0}{2k_0^2}\sum_k\left(\frac{\partial}{\partial r_k}\epsilon_r^{-1}\frac{\partial}{\partial r_k}-\frac{\partial}{\partial r_k'}\epsilon_r^{-1}\frac{\partial}{\partial r_k'}\right)\\&\quad\times I_{ij}(\mathbf{r};\mathbf{r}')+i\frac{\omega_0}{2k_0^2}\sum_k\left(\frac{\partial}{\partial r_i}\epsilon_r^{-1}\frac{\partial}{\partial r_k}\right.\\&\quad\left.\times I_{kj}(\mathbf{r};\mathbf{r}')-\frac{\partial}{\partial r_j'}\epsilon_r^{-1}\frac{\partial}{\partial r_k'}I_{ik}(\mathbf{r};\mathbf{r}')\right)\\&\quad-ig_0\frac{\sqrt{\nu_0}}{8\pi^3}\int d^3\mathbf{k}(C_{ij}(\mathbf{r};\mathbf{r}',\mathbf{k})-C_{ji}^*(\mathbf{r}';\mathbf{r},\mathbf{k})),\end{aligned} \tag{31c}$$

$$\begin{aligned}\frac{\partial}{\partial t}p_i(\mathbf{r},\mathbf{k})&=-[\Gamma(\mathbf{k})+i\Omega(\mathbf{k})]p_i(\mathbf{r},\mathbf{k})\\&\quad+ig_0\frac{2\sqrt{\nu_0}}{3}[f_{eq}^e(k;N(\mathbf{r}))\\&\quad+f_{eq}^h(k;N(\mathbf{r}))-1]\mathcal{E}_i(\mathbf{r}),\end{aligned} \tag{31d}$$

$$\begin{aligned}\frac{\partial}{\partial t}\mathcal{E}_i(\mathbf{r})&=i\frac{\omega_0}{2k_0^2}\Bigg(\sum_k\frac{\partial}{\partial r_k}\epsilon_r^{-1}\frac{\partial}{\partial r_k}\mathcal{E}_i(\mathbf{r})\\&\quad-\frac{\partial}{\partial r_i}\epsilon_r^{-1}\frac{\partial}{\partial r_k}\mathcal{E}_k(\mathbf{r})+k_0^2\mathcal{E}_i(\mathbf{r})\Bigg)\\&\quad-ig_0\frac{\sqrt{\nu_0}}{8\pi^3}\int d^3\mathbf{k}p_i(\mathbf{r},\mathbf{k}).\end{aligned} \tag{31e}$$

In order to describe a realistic diode one needs to describe not only the volume of the active region but also the propagation of light out of this region. This may either be achieved by defining realistic boundary conditions or by setting all material properties equal to zero outside a finite active volume and calculating the light field propagation into the outside medium by varying ϵ_r in space.

B. Three-dimensional quantum Maxwell-Bloch equations for quantum wells

Next, we will formulate the equations for a quantum well structure. For this case, we will also describe different cavity structures and the appropriate paraxial approximations possible for the various types of laser devices. Using the terminology of Eqs. (14a–14f), the quantum Maxwell-Bloch equations for a multi-quantum-well structure with Q quantum wells read

$$\begin{aligned}\frac{\partial}{\partial t}N(\mathbf{r}_\parallel)&=D_{amb}\Delta N(\mathbf{r}_\parallel)+j(\mathbf{r}_\parallel)-\gamma N(\mathbf{r}_\parallel)\\&\quad+ig_0\frac{\sqrt{\nu_0}}{4\pi^2}\int d^2\mathbf{k}_\parallel\sum_i\,(C_{ii_\parallel}(\mathbf{r};\mathbf{r}_\parallel,\mathbf{k}_\parallel)_{r_z=z_0}\\&\quad-C_{ii_\parallel}^*(\mathbf{r};\mathbf{r}_\parallel,\mathbf{k}_\parallel)_{r_z=z_0}),\end{aligned} \tag{32a}$$

$$\begin{aligned}\frac{\partial}{\partial t}C_{ij_\parallel}(\mathbf{r};\mathbf{r}'_\parallel,\mathbf{k}_\parallel)&=-[\Gamma(\mathbf{k}_\parallel)+i\Omega(\mathbf{k}_\parallel)]C_{ij_\parallel}(\mathbf{r};\mathbf{r}'_\parallel,\mathbf{k}_\parallel)\\&\quad-i\frac{\omega_0}{2k_0^2}\Bigg(\sum_k\frac{\partial}{\partial r_k}\epsilon_r^{-1}\frac{\partial}{\partial r_k}C_{ij_\parallel}(\mathbf{r};\mathbf{r}'_\parallel,\mathbf{k}_\parallel)\\&\quad-\sum_k\frac{\partial}{\partial r_i}\epsilon_r^{-1}\frac{\partial}{\partial r_k}C_{kj_\parallel}(\mathbf{r};\mathbf{r}'_\parallel,\mathbf{k}_\parallel)+k_0^2C_{ij_\parallel}(\mathbf{r};\mathbf{r}'_\parallel,\mathbf{k}_\parallel)\Bigg)\\&\quad+ig_0Q\sqrt{\nu_0}\left[f_{eq}^e\left(k_\parallel;\frac{N(\mathbf{r}'_\parallel)}{Q}\right)+f_{eq}^h\left(k_\parallel;\frac{N(\mathbf{r}'_\parallel)}{Q}\right)-1\right]\\&\quad\times I_{ij}(\mathbf{r};\mathbf{r}')_{r'_z=z_0}+ig_0Q\sqrt{\nu_0}\delta(\mathbf{r}_\parallel-\mathbf{r}'_\parallel)\,\delta(r_z-z_0)\\&\quad\times\delta_{ij_\parallel}f_{eq}^e\left(k_\parallel;\frac{N(\mathbf{r}_\parallel)}{Q}\right)f_{eq}^h\left(k_\parallel;\frac{N(\mathbf{r}_\parallel)}{Q}\right).\end{aligned} \tag{32b}$$

$$\begin{aligned}\frac{\partial}{\partial t}I_{ij}(\mathbf{r};\mathbf{r}')&=-i\frac{\omega_0}{2k_0^2}\sum_k\left(\frac{\partial}{\partial r_k}\epsilon_r^{-1}\frac{\partial}{\partial r_k}-\frac{\partial}{\partial r_k'}\epsilon_r^{-1}\frac{\partial}{\partial r_k'}\right)\\&\quad\times I_{ij}(\mathbf{r};\mathbf{r}')+i\frac{\omega_0}{2k_0^2}\sum_k\left(\frac{\partial}{\partial r_i}\epsilon_r^{-1}\frac{\partial}{\partial r_k}I_{kj}(\mathbf{r};\mathbf{r}')\right.\\&\quad\left.-\frac{\partial}{\partial r_j'}\epsilon_r^{-1}\frac{\partial}{\partial r_k'}I_{ik}(\mathbf{r};\mathbf{r}')\right)-ig_0\frac{\sqrt{\nu_0}}{4\pi^2}\\&\quad\times\int d^2\mathbf{k}_\parallel(C_{ij_\parallel}(\mathbf{r};\mathbf{r}'_\parallel,\mathbf{k}_\parallel)\,\delta(r'_z-z_0)\\&\quad-C_{ji_\parallel}^*(\mathbf{r}';\mathbf{r}_\parallel,\mathbf{k}_\parallel)\,\delta(r_z-z_0)),\end{aligned} \tag{32c}$$

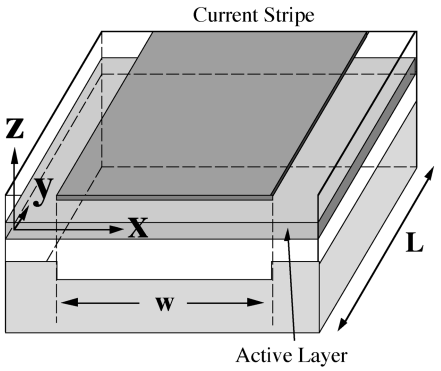

FIG. 1. Schematic representation of the edge emitter geometry. The laser field is mostly confined to the plane of the quantum well and propagates along the y axis.

$$\frac{\partial}{\partial t}p_{i_\parallel}(\mathbf{r}_\parallel,\mathbf{k}_\parallel)=-(\Gamma(\mathbf{k}_\parallel)+i\Omega(\mathbf{k}_\parallel))p_{i_\parallel}(\mathbf{r}_\parallel,\mathbf{k}_\parallel)+ig_0Q\sqrt{\nu_0}\left[f^e_{eq}\left(k_\parallel;\frac{N(\mathbf{r}_\parallel)}{Q}\right)+f^h_{eq}\left(k_\parallel;\frac{N(\mathbf{r}_\parallel)}{Q}\right)-1\right]\mathcal{E}_i(\mathbf{r})_{r_z=z_0}, \quad (32d)$$

$$\frac{\partial}{\partial t}\mathcal{E}_i(\mathbf{r})=i\frac{\omega_0}{2k_0^2}\left(\sum_k\frac{\partial}{\partial r_k}\epsilon_r^{-1}\frac{\partial}{\partial r_k}\mathcal{E}_i(\mathbf{r})-\frac{\partial}{\partial r_i}\epsilon_r^{-1}\frac{\partial}{\partial r_k}\mathcal{E}_k(\mathbf{r})+k_0^2\mathcal{E}_i(\mathbf{r})\right)-ig_0\frac{\sqrt{\nu_0}}{4\pi^2}\int d^2\mathbf{k}_\parallel p_{i_\parallel}(\mathbf{r}_\parallel,\mathbf{k}_\parallel)\delta(r_z-z_0). \quad (32e)$$

Note that $N(\mathbf{r}_\parallel)$ is the total carrier density. Therefore, the density per quantum well that determines the chemical potential of the carrier distribution functions is $N(\mathbf{r}_\parallel)/Q$. Again, the structure of an external cavity may be considered either by boundary conditions or by spatially varying ϵ_r. In particular, laser diodes may be described by distinguishing between reflective and nonreflective edges. If the reflective surface is perpendicular to the plane of the quantum wells, the laser is an edge emitter. If the reflectivity is very high on the surface planes parallel to the quantum wells, the laser is a vertical cavity surface emitting laser (VCSEL).

C. One-dimensional quantum Maxwell-Bloch equations for edge emitting lasers

In an edge emitting laser, the laser light field propagates in the plane of the quantum well. Since the z direction is already defined as the one perpendicular to the quantum well we will define the y direction as the direction along which the laser light propagates. A schematic representation of this type of laser geometry is shown in Fig. 1. It is possible to drastically reduce the dimensionality of the equation describing the edge emitting laser geometry by noting that the light field polarization of the amplified fields will be in the plane of the quantum well and by limiting the analysis to a single longitudinal mode. Effectively, this corresponds to a light field $\mathcal{E}(\mathbf{r})$ with the following properties:

$$\mathcal{E}_x(\mathbf{r}):=\mathcal{E}_0(r_x)\xi(r_y,r_z), \quad (33a)$$

$$\mathcal{E}_z(\mathbf{r}):=0, \quad (33b)$$

$$\frac{\partial}{\partial r_y}\mathcal{E}_y(\mathbf{r}):=-\frac{\partial}{\partial r_x}\mathcal{E}_x(\mathbf{r}). \quad (33c)$$

The envelope function $\xi(r_y,r_z)$ describes both the propagation along the y direction and the confinement along the z direction. It represents an approximate solution of the wave equation in the yz plane normalized by

$$\int dr_y dr_z|\xi(r_y,r_z)|^2=1. \quad (33d)$$

The equations are then limited to light field modes with the two-dimensional envelope $\xi(r_y,r_z)$. Spontaneous emission into other light field modes must be considered by including the rate of emission in the carrier recombination rate γ. Since the length L of the laser in the y direction is also an important property of the device, it is included by considering the openness of the optical cavity. With the reflectivities of the laser mirrors given by R_1 and R_2, the light field in the cavity is damped by losses through the mirrors at a rate of

$$\kappa=-\frac{c}{2L\sqrt{\epsilon_r}}\ln[R_1R_2]. \quad (34)$$

The new one-dimensional variables are now defined as follows:

$$N_{1D}(r_x)=\int dr_y N(\mathbf{r}_\parallel), \quad (35a)$$

$$C_0(r_x;r_x',\mathbf{k}_\parallel)=\int dr_y dr_z dr_y'\xi(r_y,r_z)\times\xi^*(r_y',r_z'=z_0)C_{xx}(\mathbf{r};\mathbf{r}'_\parallel,\mathbf{k}_\parallel), \quad (35b)$$

$$I_0(r_x;r_x')=\int dr_y dr_z dr_y' dr_z'\xi(r_y,r_z)\xi^*(r_y',r_z')I_{xx}(\mathbf{r};\mathbf{r}'), \quad (35c)$$

$$p_0(r_x,\mathbf{k}_\parallel)=\int dr_y\xi^*(r_y,r_z=z_0)p_x(\mathbf{r}_\parallel,\mathbf{k}_\parallel), \quad (35d)$$

$$\mathcal{E}_0(r_x)=\int dr_y dr_z\xi^*(r_y,r_z)\mathcal{E}_x(\mathbf{r}). \quad (35e)$$

The carrier density is now given in terms of a one-dimensional density. To obtain the two-dimensional carrier density per quantum well, this density is to be divided by QL. Note that the intensity is also given in terms of photons per unit length. The dynamics of the edge emitter then reads

$$\frac{\partial}{\partial t}N_{1D}(r_x)=D_{amb}\frac{\partial^2}{\partial r_x^2}N_{1D}(r_x)+Lj(r_x)-\gamma N_{1D}(r_x)+ig_0\frac{\sqrt{\nu_0}}{4\pi^2}\int d^2\mathbf{k}_\parallel(C_0(r_x;r_x,\mathbf{k}_\parallel)-C_0^*(r_x;r_x,\mathbf{k}_\parallel)), \tag{36a}$$

$$\frac{\partial}{\partial t}C_0(r_x;r_x',\mathbf{k}_\parallel)=-[\Gamma(\mathbf{k}_\parallel)+i\Omega(\mathbf{k}_\parallel)]C_0(r_x;r_x',\mathbf{k}_\parallel)-\kappa C_0(r_x;r_x',\mathbf{k}_\parallel)-i\frac{\omega_0}{2k_0^2\epsilon_r}\frac{\partial^2}{\partial r_x^2}C_0(r_x;r_x',\mathbf{k}_\parallel)+ig_0\sigma\sqrt{\nu_0}\left[f_{eq}^e\left(k_\parallel;\frac{N_{1D}(r_x')}{QL}\right)+f_{eq}^h\left(k_\parallel;\frac{N_{1D}(r_x')}{QL}\right)-1\right]I_0(r_x;r_x')+ig_0\sigma\sqrt{\nu_0}\delta(r_x-r_x')\times f_{eq}^e\left(k_\parallel;\frac{N_{1D}(r_x)}{QL}\right)f_{eq}^h\left(k_\parallel;\frac{N_{1D}(r_x)}{QL}\right), \tag{36b}$$

$$\frac{\partial}{\partial t}I_0(r_x;r_x')=-2\kappa I_0(r_x;r_x')-i\frac{\omega_0}{2k_0^2\epsilon_r}\left(\frac{\partial^2}{\partial r_x^2}-\frac{\partial^2}{\partial r_x'^2}\right)I_0(r_x;r_x')-ig_0\frac{\sqrt{\nu_0}}{4\pi^2}\int d^2\mathbf{k}_\parallel(C_0(r_x;r_x',\mathbf{k}_\parallel)-C_0^*(r_x';r_x,\mathbf{k}_\parallel)). \tag{36c}$$

$$\frac{\partial}{\partial t}p_0(r_x,\mathbf{k}_\parallel)=-(\Gamma(\mathbf{k}_\parallel)+i\Omega(\mathbf{k}_\parallel))p_0(r_x,\mathbf{k}_\parallel)+ig_0\sigma\sqrt{\nu_0}\left[f_{eq}^e\left(k_\parallel;\frac{N_{1D}(r_x)}{QL}\right)+f_{eq}^h\left(k_\parallel;\frac{N_{1D}(r_x)}{QL}\right)-1\right]\mathcal{E}_0(r_x), \tag{36d}$$

$$\frac{\partial}{\partial t}\mathcal{E}_0(r_x)=-\kappa\mathcal{E}_0(r_x)+i\frac{\omega_0}{2k_0^2\epsilon_r}\frac{\partial^2}{\partial r_x^2}\mathcal{E}_0(r_x)-ig_0\frac{\sqrt{\nu_0}}{4\pi^2}\int d^2\mathbf{k}_\parallel p_0(r_x,\mathbf{k}_\parallel), \tag{36e}$$

where σ is the confinement factor that determines the overlap between the quantum wells and the light field mode,

$$\sigma=Q\int dr_y|\xi(r_y,r_z=z_0)|^2. \tag{37}$$

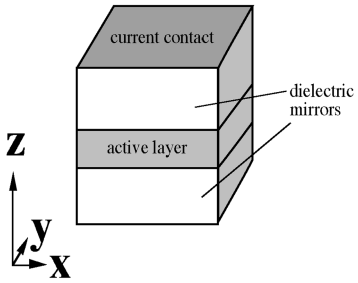

FIG. 2. Schematic representation of a typical VCSEL geometry. The laser field propagates perpendicularly to the quantum well along the z axis. The length of the optical resonator approximately corresponds to the wavelenth.

D. Two-dimensional quantum Maxwell-Bloch equations for VCSEL's

In a VCSEL the light field is strongly confined by highly reflective mirrors above and below the quantum wells. The light field propagates perpendicular to the quantum well structure as shown in Fig. 2. Therefore both the possible polarization directions and the spatial dynamics remain two dimensional. Only the z direction may be eliminated by averaging over a single longitudinal mode. Coupling terms between the polarization directions should be taken into account, even if they are small. For VCSEL's, the assumptions read

$$\mathcal{E}(\mathbf{r})\approx\tilde{\mathcal{E}}(\mathbf{r}_\parallel)\xi(r_z), \tag{38a}$$

$$\frac{\partial}{\partial r_z}\mathcal{E}_z(\mathbf{r})\approx-\frac{\partial}{\partial r_x}\left(\mathcal{E}_x(\mathbf{r})+\frac{2g_0\sqrt{\nu_0}}{4\pi\omega_0}\times\int d^2\mathbf{k}_\parallel\delta(r_z-z_0)p_x(\mathbf{r}_\parallel,\mathbf{k}_\parallel)\right)-\frac{\partial}{\partial r_y}\left(\mathcal{E}_y(\mathbf{r})+\frac{2g_0\sqrt{\nu_0}}{4\pi\omega_0}\times\int d^2\mathbf{k}_\parallel\delta(r_z-z_0)p_y(\mathbf{r}_\parallel,\mathbf{k}_\parallel)\right). \tag{38b}$$

The latter condition takes into account the divergence of $\mathcal{E}(\mathbf{r})$ caused by the polarization $\mathbf{p}_\parallel(\mathbf{r}_\parallel,\mathbf{k}_\parallel)$. This is an important contribution to the quantum Maxwell-Bloch equations, since it coherently couples orthogonal polarizations. The properties of the envelope function $\xi(r_z)$ are defined as

$$\int dr_z|\xi(r_z)|^2=1, \tag{38c}$$

$$\frac{\partial^2}{\partial r_z^2}\xi(r_z)\approx-k_0^2\xi(r_z). \tag{38d}$$

The cavity loss rate κ is defined as in Eq. (34). However, the experimentally observed polarization stability is taken into account by using slightly different reflectivities for the x and y polarizations. The cavity loss rate is therefore given by κ_x and κ_y. Experimental results [20] suggest that $(\kappa_y-\kappa_x)/(\kappa_x)\approx10^{-3}-10^{-2}$. A birefringence of $\delta\omega_{x/y}$ is also

included to denote the difference between the band-gap frequency and the longitudinal frequencies of the confined light field for the two polarization directions. The birefringence $\delta\omega_x - \delta\omega_y$ is usually in the GHz range. Since all coordinates are two dimensional, the index $_\parallel$ that marked the two-dimensional coordinates in the quantum well equations will be omitted. Instead, the two-dimensional variables are marked with a tilde. All indices and coordinates of such variables are only defined in two dimensions. The variables are defined as

$$\tilde{N}(\mathbf{r}) = N(\mathbf{r}_\parallel), \tag{39a}$$

$$\tilde{C}_{ij}(\mathbf{r};\mathbf{r}',\mathbf{k}) = \int dr_z \xi(r_z)\xi^*(r_z'=z_0) C_{ij_\parallel}(\mathbf{r};\mathbf{r}'_\parallel,\mathbf{k}_\parallel), \tag{39b}$$

$$\tilde{I}_{ij}(\mathbf{r};\mathbf{r}') = \int dr_z dr_z' \xi(r_z)\xi^*(r_z') I_{ij}(\mathbf{r};\mathbf{r}'), \tag{39c}$$

$$\tilde{p}_i(\mathbf{r},\mathbf{k}) = \xi^*(r_z=z_0) p_{i_\parallel}(\mathbf{r}_\parallel,\mathbf{k}_\parallel), \tag{39d}$$

$$\tilde{\mathcal{E}}_i(\mathbf{r}) = \int dr_z \xi^*(r_z)\mathcal{E}_i(\mathbf{r}). \tag{39e}$$

Note that the dipole variable $p_{i_\parallel}(\mathbf{r}_\parallel,\mathbf{k}_\parallel)$ is rescaled by the field density of the envelope function $\xi(r_z)$ at $r_z = z_0$. The dipole given by $\tilde{p}_i(\mathbf{r},\mathbf{k})$ is therefore the average dipole density within the whole cavity, not just within the quantum wells. The quantum Maxwell-Bloch equations for the VCSEL now read

$$\begin{aligned}\frac{\partial}{\partial t}\tilde{N}(\mathbf{r}) &= D_{amb}\Delta\tilde{N}(\mathbf{r}) + \tilde{j}(\mathbf{r}) - \gamma\tilde{N}(\mathbf{r}) \\ &\quad + ig_0\frac{\sqrt{\nu_0}}{4\pi^2}\int d^2\mathbf{k} \\ &\quad \times\Bigg(\sum_i [\tilde{C}_{ii}(\mathbf{r};\mathbf{r},\mathbf{k}) - \tilde{C}^*_{ii}(\mathbf{r};\mathbf{r},\mathbf{k})] \\ &\quad + \sum_{ij}\frac{1}{k_0^2\epsilon_r}\int d^2\mathbf{r}'\,\delta(\mathbf{r}-\mathbf{r}') \\ &\quad \times\left(\frac{\partial^2}{\partial r_i' r_j'}\tilde{C}_{ij}(\mathbf{r};\mathbf{r}',\mathbf{k}) - \frac{\partial^2}{\partial r_i r_j}\tilde{C}^*_{ij}(\mathbf{r}';\mathbf{r},\mathbf{k})\right)\Bigg),\end{aligned} \tag{40a}$$

$$\begin{aligned}\frac{\partial}{\partial t}\tilde{C}_{ij}(\mathbf{r};\mathbf{r}',\mathbf{k}) &= -[\Gamma(\mathbf{k}) + i\Omega(\mathbf{k})]\tilde{C}_{ij}(\mathbf{r};\mathbf{r}',\mathbf{k}) \\ &\quad - (\kappa_i - i\delta\omega_i)\tilde{C}_{ij}(\mathbf{r};\mathbf{r}',\mathbf{k}) - i\frac{\omega_0}{2k_0^2\epsilon_r}\Delta_{\mathbf{r}}\tilde{C}_{ij}(\mathbf{r};\mathbf{r}',\mathbf{k}) \\ &\quad + ig_0\sigma\sqrt{\nu_0}\Bigg[f^e_{eq}\left(k;\frac{\tilde{N}(\mathbf{r}')}{Q}\right) \\ &\quad + f^h_{eq}\left(k;\frac{\tilde{N}(\mathbf{r}')}{Q}\right) - 1\Bigg]\tilde{I}_{ij}(\mathbf{r};\mathbf{r}') \\ &\quad + ig_0\sigma\sqrt{\nu_0}\delta(\mathbf{r}-\mathbf{r}')\,\delta_{ij} f^e_{eq}\left(k;\frac{\tilde{N}(\mathbf{r})}{Q}\right) f^h_{eq}\left(k;\frac{\tilde{N}(\mathbf{r})}{Q}\right),\end{aligned} \tag{40b}$$

$$\begin{aligned}\frac{\partial}{\partial t}\tilde{I}_{ij}(\mathbf{r};\mathbf{r}') &= -(\kappa_i + \kappa_j)\tilde{I}_{ij}(\mathbf{r};\mathbf{r}') - i\frac{\omega_0}{2k_0^2\epsilon_r}(\Delta_{\mathbf{r}} - \Delta_{\mathbf{r}'})\tilde{I}_{ij}(\mathbf{r};\mathbf{r}') \\ &\quad - ig_0\frac{\sqrt{\nu_0}}{4\pi^2}\int d^2\mathbf{k}\Bigg(\tilde{C}_{ij}(\mathbf{r};\mathbf{r}',\mathbf{k}) - \tilde{C}^*_{ji}(\mathbf{r}';\mathbf{r},\mathbf{k}) \\ &\quad + \sum_k\frac{1}{k_0^2\epsilon_r}\left(\frac{\partial^2}{\partial r_j' r_k'}\tilde{C}_{ik}(\mathbf{r};\mathbf{r}',\mathbf{k}) - \frac{\partial^2}{\partial r_i r_k}\tilde{C}^*_{jk}(\mathbf{r}';\mathbf{r},\mathbf{k})\right)\Bigg),\end{aligned} \tag{40c}$$

$$\begin{aligned}\frac{\partial}{\partial t}\tilde{p}_i(\mathbf{r},\mathbf{k}) &= -[\Gamma(\mathbf{k}) + i\Omega(\mathbf{k})]\tilde{p}_i(\mathbf{r},\mathbf{k}) \\ &\quad + ig_0\sigma\sqrt{\nu_0}\Bigg[f^e_{eq}\left(k;\frac{\tilde{N}(\mathbf{r})}{Q}\right) \\ &\quad + f^h_{eq}\left(k;\frac{\tilde{N}(\mathbf{r})}{Q}\right) - 1\Bigg]\tilde{\mathcal{E}}_i(\mathbf{r}),\end{aligned} \tag{40d}$$

$$\begin{aligned}\frac{\partial}{\partial t}\tilde{\mathcal{E}}_i(\mathbf{r}) &= -(\kappa_i + i\delta\omega_i)\tilde{\mathcal{E}}_i(\mathbf{r}) + i\frac{\omega_0}{2k_0^2\epsilon_r}\Delta\tilde{\mathcal{E}}_i(\mathbf{r}) \\ &\quad - ig_0\frac{\sqrt{\nu_0}}{4\pi^2}\int d^2\mathbf{k}\Bigg(\tilde{p}_i(\mathbf{r},\mathbf{k}) \\ &\quad + \sum_j\frac{1}{k_0^2\epsilon_r}\frac{\partial^2}{\partial r_i r_j}\tilde{p}_j(\mathbf{r},\mathbf{k})\Bigg),\end{aligned} \tag{40e}$$

with σ being the confinement factor along the z direction,

$$\sigma = Q|\xi(r_z=z_0)|^2. \tag{41}$$

Equations (40) present a starting point for the study of spatial polarization patterns and fluctuations in VCSEL's. For more realistic models, it may also be desirable to include a spatial

dependence of the birefringence and the dichroism. Also, nonlinear effects may be introduced, e.g., by separating the carrier densities for right and left circular polarization [15].

E. Statistical interpretation and two-time correlations

Using the equations presented above, it is now possible to calculate the emergence of a spatially coherent light field in semiconductor laser diodes both above and below threshold. Note that the average light field $\mathbf{E}(\mathbf{r})$ will remain zero at all times due to the random phases of spontaneous emission processes. The (average) spatial coherence of the light field, however, does not vanish and is fully described by the nonlocal field-field correlations $\mathbf{I}(\mathbf{r};\mathbf{r}')$, which emerge due to the propagation and/or amplification of the originally incoherent local spontaneous emissions. This emergence of coherence as a concequence of incoherent emissions has been discussed in a temporal context using nonequilibrium Green's functions in [11].

In order to understand the physical implications of the well known absence of an average light field in lasers, it should be recalled that all the results of the quantum Maxwell-Bloch equations represent averages that have to be interpreted in terms of statistical physics. For example, the field-field correlation $\mathbf{I}(\mathbf{r};\mathbf{r}')$ represents a variance of the probability distribution with respect to the possible spatial electromagnetic field values. The coherent field observed in experimental time-resolved measurements will vary randomly from measurement to measurement according to this probability distribution. Indeed, the intensity distribution itself will vary depending on the random phase interference of the eigenmodes given by $\mathbf{I}(\mathbf{r};\mathbf{r}')$. The calculated average spatial intensity distribution $\mathbf{I}(\mathbf{r};\mathbf{r})$ only describes the average near field pattern, which is likely to be close to but not identical with the one actually observed. The fluctuations of the actual intensity distribution around this average, however, are disregarded as a consequence of the factorization performed in Sec. II. Moreover, the fluctuations in the carrier density distribution induced by spatial hole burning associated with these fluctuations of the intensity distribution have also been disregarded.

While the average spatial coherence of the light field is fully described by the quantum Maxwell-Bloch equations, the average expected temporal coherence has not yet been explicitly considered. Indeed, it is not necessary to consider temporal coherence in the closed sets of quantum Maxwell-Bloch equations given above because all the information required to obtain the correct emission and absorption rates are incorporated in the field-dipole correlation $\mathbf{C}(\mathbf{r};\mathbf{r}',\mathbf{k})$. As shown in Sec. VI, the spectra of gain and spontaneous emission are implicitly given by the coherent dipole dynamics, which enters into the temporal evolution of this field-dipole correlation. If explicit information about the two-time correlations is desired, however, such correlations may be included in the dynamics by noting that the temporal evolution of the two-time correlations of the field $\mathbf{I}(\mathbf{r},t;\mathbf{r}',t')$ and the two-time correlations of the field-dipole correlation $\mathbf{C}(\mathbf{r},t;\mathbf{r}',\mathbf{k},t')$ is equivalent to the dynamics of the field and dipole expectation values [25]. While the quantum Maxwell-Bloch equations for the correlations at $t=t'$ remain unchanged, the evolution of the two time correlations as a function of $t'>t$ is then given by an additional pair of equations that depends on the carrier dynamics given by the solution of the original system of quantum Maxwell-Bloch equations as presented above. In the case of VCSEL's these additional equations supplementing Eqs. (40) read

$$\begin{aligned}\frac{\partial}{\partial t'}\tilde{C}_{ij}(\mathbf{r},t;\mathbf{r}',\mathbf{k},t') &= -(\Gamma(\mathbf{k})+i\Omega(\mathbf{k}))\tilde{C}_{ij}(\mathbf{r},t;\mathbf{r}',\mathbf{k},t') \\ &\quad + ig_0\sigma\sqrt{\nu_0}\left[f^e_{eq}\left(k;\frac{\tilde{N}(\mathbf{r},t')}{Q}\right)\right. \\ &\quad \left. + f^h_{eq}\left(k;\frac{\tilde{N}(\mathbf{r},t')}{Q}\right)-1\right]\tilde{I}_{ij}(\mathbf{r},t;\mathbf{r}',t') \qquad (42a)\end{aligned}$$

$$\begin{aligned}\frac{\partial}{\partial t'}\tilde{I}_{ij}(\mathbf{r},t;\mathbf{r}',t') &= -(\kappa_j+i\delta\omega_j)\tilde{I}_{ij}(\mathbf{r},t;\mathbf{r}',t') \\ &\quad + i\frac{\omega_0}{2k_0^2\epsilon_r}\Delta_{\mathbf{r}'}\tilde{I}_{ij}(\mathbf{r},t;\mathbf{r}',t') \\ &\quad - ig_0\frac{\sqrt{\nu_0}}{4\pi^2}\int d^2\mathbf{k}\tilde{C}_{ij}(\mathbf{r},t;\mathbf{r}',\mathbf{k},t') \\ &\quad - ig_0\frac{\sqrt{\nu_0}}{4\pi^2}\int d^2\mathbf{k}\sum_k \frac{1}{k_0^2\epsilon_r}\frac{\partial^2}{\partial r'_j r'_k}\tilde{C}_{ik}(\mathbf{r},t;\mathbf{r}',\mathbf{k},t'). \qquad (42b)\end{aligned}$$

If the carrier density changes slowly, the equations describe the linear response of the medium caused by the initial intensity distribution $\tilde{I}_{ij}(\mathbf{r},t;\mathbf{r}',t)$ and the initial field-dipole correlation $\tilde{C}_{ij}(\mathbf{r},t;\mathbf{r}',\mathbf{k},t)$ determined from Eqs. (40). In this case it is possible to derive the spectrum and the gain from the eigenmodes and the associated eigenvalues of the quasistationary linear optical system. Note that the eigenmodes of the linearized dynamics are not necessarily identical with the eigenmodes of the intensity distribution $\tilde{I}_{ij}(\mathbf{r},t;\mathbf{r}',t)$, since fast variations in the carrier density distribution may have induced phase locking between the dynamical eigenmodes.

In general, the frequency spectra of the light field are given by Fourier transforms of the two-time correlations obtained from Eqs. (42). However, as noted above, such spectra do not comprise any effects which arise from carrier density fluctuations. These effects are known to be quite significant. Well known examples of carrier fluctuation effects in the frequency spectrum of semiconductor lasers are the linewidth enhancement phenomenologically described by the linewidth enhancement factor α and the relaxation oscillation sidebands observed in stable single mode operation. Moreover, spatial carrier density fluctuations may also significantly modify the multimode spectra of semiconductor laser devices, as pointed out recently for the case of semiconductor laser arrays [24].

VI. AMPLIFIED SPONTANEOUS EMISSION PROPERTIES: ANALYTICAL RESULTS OF THE QUANTUM MAXWELL-BLOCH EQUATIONS

A. Gain and spontaneous emission

For a given carrier distribution $f^{e/h}(k)$, the dynamics of the optical field $\mathcal{E}(\mathbf{r})$ and the dipole density $\mathbf{p}(\mathbf{r})$ are linear. In this case, it is possible to integrate the equations of motion to obtain a Green's function for the field dynamics. The equation for bulk material reads

$$\left.\frac{\partial}{\partial t}\mathcal{E}(\mathbf{r},t)\right|_{cL} = g_0^2\frac{\nu_0}{12\pi^3}\int d^3\mathbf{k}\int_0^\infty d\tau e^{-[\Gamma(\mathbf{k})+i\Omega(\mathbf{k})]\tau} \times (f^e(k)+f^h(k)-1)\mathcal{E}(\mathbf{r},t-\tau). \tag{43a}$$

Correspondingly, the equation for a multi-quantum-well structure of Q quantum wells has the form

$$\left.\frac{\partial}{\partial t}\mathcal{E}(\mathbf{r},t)\right|_{cL} = g_0^2\frac{Q\nu_0}{4\pi^2}\delta(r_z-z_0)\int d^2\mathbf{k}_\parallel\int_0^\infty d\tau e^{-(\Gamma(\mathbf{k}_\parallel)+i\Omega(\mathbf{k}_\parallel))\tau} \times (f^e(k_\parallel)+f^h(k_\parallel)-1)\mathcal{E}(\mathbf{r},t-\tau). \tag{43b}$$

An expression for the rate $G(\omega)$ at which a light field mode of frequency ω is amplified can be derived by solving the integral over τ using $\mathcal{E}(\mathbf{r},t-\tau)\approx e^{i\omega\tau}\mathcal{E}(\mathbf{r},t)$. The real part of the result is the gain spectrum given in terms of amplification per unit time, $G(\omega)$. For bulk material, this amplification rate is given by

$$G_{bulk}(\omega) = g_0^2\frac{\nu_0}{12\pi^3}\int d^3\mathbf{k}\frac{\Gamma(\mathbf{k})}{\Gamma^2(\mathbf{k})+(\Omega(\mathbf{k})-\omega)^2} \times [f^e(k)+f^h(k)-1], \tag{44a}$$

and for quantum wells, the corresponding amplification rate reads

$$G_{QW}(\omega) = g_0^2\frac{Q\nu_0}{4\pi^2}\delta(r_z-z_0) \times\int d^2\mathbf{k}_\parallel\frac{\Gamma(\mathbf{k}_\parallel)}{\Gamma^2(\mathbf{k}_\parallel)+(\Omega(\mathbf{k}_\parallel)-\omega)^2} \times [f^e(k_\parallel)+f^h(k_\parallel)-1]. \tag{44b}$$

The gain per unit length can be obtained by dividing the rate $G(\omega)$ by the speed of light in the semiconductor medium, $c\epsilon_r^{-1/2}$. However, in order to establish the connection between the gain spectrum and the spectral density of spontaneous emission, it is more convenient to use the amplification rate as a starting point.

The quantum Maxwell-Bloch equations for the field-dipole correlation $C_{ij}(\mathbf{r};\mathbf{r}',\mathbf{k})$ show that the ratio between the spontaneous contributions and the stimulated contributions is

$$\frac{\left.\frac{\partial}{\partial t}C_{ij}(\mathbf{r};\mathbf{r}',\mathbf{k})\right|_{spontaneous}}{\left.\frac{\partial}{\partial t}C_{ij}(\mathbf{r};\mathbf{r}',\mathbf{k})\right|_{stimulated}} = \frac{\delta(\mathbf{r}-\mathbf{r}')\delta_{ij}f^e(k)f^h(k)}{I_{ij}(\mathbf{r};\mathbf{r}')[f^e(k)+f^h(k)-1]}. \tag{45}$$

In this equation, $\delta(\mathbf{r}-\mathbf{r}')\delta_{ij}$ corresponds to a photon density of one photon per mode. The spectral density of the spontaneous emission may therefore be obtained by replacing $[f^e(k)+f^h(k)-1]$ with $f^e(k)f^h(k)$ in Eqs. (44a) and (44b), respectively, and multiplying the resulting rates with twice the density of light field modes that couple to the medium (the factor of 2 being a result of considering intensities instead of fields). At the band edge frequency ω_0, the density of light field modes per volume and frequency interval in a continuous medium is

$$\rho_{light} = \frac{\omega_0^2}{\pi^2c^3}\epsilon_r^{3/2}. \tag{46}$$

The density of the spontaneous emission rate for bulk material $S_{bulk}(\omega)$ thus reads

$$S_{bulk}(\omega) = \rho_{light}g_0^2\frac{\nu_0}{6\pi^3} \times\int d^3\mathbf{k}\frac{\Gamma(\mathbf{k})}{\Gamma^2(\mathbf{k})+(\Omega(\mathbf{k})-\omega)^2}f^e(k)f^h(k). \tag{47a}$$

For quantum wells, the density of modes is only 2/3 of ρ_{light}, since the dipole component perpendicular to the quantum well is zero. Also, the δ function $\delta(r_z-z_0)$ may be omitted to obtain the emission density per area. The spontaneous emission density $S_{QW}(\omega)$ is then given by

$$S_{QW}(\omega) = \frac{2}{3}\rho_{light}g_0^2\frac{Q\nu_0}{2\pi^2}\delta(r_z-z_0) \times\int d^2\mathbf{k}_\parallel\frac{\Gamma(\mathbf{k}_\parallel)}{\Gamma^2(\mathbf{k}_\parallel)+(\Omega(\mathbf{k}_\parallel)-\omega)^2}f^e(k_\parallel)f^h(k_\parallel). \tag{47b}$$

The total rate of spontaneous emission per unit volume or area may be obtained by integrating over all frequencies. This integral removes the dependence on $\Gamma(\mathbf{k})$. For bulk material,

$$\int d\omega S_{bulk}(\omega) = \rho_{light}g_0^2\frac{\nu_0}{6\pi^2}\int d^3\mathbf{k}f^e(k)f^h(k) \tag{48a}$$

and for quantum wells,

$$\int d\omega S_{QW}(\omega) = \rho_{light}g_0^2\frac{Q\nu_0}{3\pi}\delta(r_z-z_0)\int d^2\mathbf{k}_\parallel f^e(k_\parallel)f^h(k_\parallel). \tag{48b}$$

For zero temperature, the spontaneous emission rate may be derived by noting that $f^e(k)f^h(k)=f^e(k)=f^h(k)$. The integral over $\mathbf{k}$ may thus be solved, resulting in

$$\int d^3\mathbf{k} f^e(k) f^h(k) = 4\pi^3 N \tag{49a}$$

for bulk material and

$$\int d^2\mathbf{k}_\parallel f^e(k_\parallel) f^h(k_\parallel) = \frac{2\pi^2}{Q} N \tag{49b}$$

for quantum wells. For both bulk and quantum wells the density of spontaneous emission now may be expressed as

$$S_{total} = \frac{N}{\tau_s}, \tag{50}$$

where $1/\tau_s$ is the rate of spontaneous emission given by

$$\frac{1}{\tau_s} = \frac{2\pi}{3} \rho_{light} g_0^2 \nu_0 . \tag{51}$$

Using Eq. (30), the rate of spontaneous emission may also be expressed in terms of the dipole matrix element d_{cv},

$$\frac{1}{\tau_s} = \frac{4}{\hbar\omega_0} \epsilon_r^{1/2} \frac{1}{4\pi\epsilon_0} \frac{\omega_0^4}{3c^3} |d_{cv}|^2 = \frac{4}{\hbar\omega_0} P_{rad}, \tag{52}$$

where P_{rad} is the classical power radiated by an oscillating dipole of the amplitude d_{cv}. Note that the factor of $4/\hbar\omega_0$ is consistent with a quantum noise interpretation of spontaneous emission such as the one represented by the semiclassical Langevin equations. According to this interpretation, the fluctuations of each dipole are given by $2|d_{cv}|^2$ because both the real and the imaginary parts of the dipole contribute. The spontaneous emission of an excited atom is then composed of one-half amplified field noise and one-half dipole fluctuations. Therefore, each one of the two dipole components contributes one-quarter of the total spontaneous emission of an excited state. Numerical values of $|\mathbf{d}_{cv}|$ and g_0 for GaAs may be determined by assuming a spontaneous lifetime of $\tau_s=3$ ns, a band gap of $\hbar\omega_0=1.5$ eV and $\epsilon_r=12$. The dipole matrix element is then $|\mathbf{d}_{cv}|=4.3\times10^{-29} Cm$ which corresponds to a distance of 2.7×10^{-10} m times the electron charge and the coupling frequency is $g_0=2.1\times10^{15}\ \mathrm{s}^{-1}$.

For quantum wells at zero temperature, the integrals over $\mathbf{k}_\parallel$ can be solved analytically using Eq. (20) and assuming that Γ is independent of $\mathbf{k}_\parallel$. The resulting gain spectrum is then given by

$$\frac{\epsilon_r^{1/2}}{c} G_{QW}(\omega) = \frac{\epsilon_r^{1/2}}{c} g_0^2 \frac{Q\nu_0}{2\pi\hbar} \frac{m^e_{eff} m^h_{eff}}{m^e_{eff}+m^h_{eff}} \delta(r_z - z_0) \times \left[2 \arctan\left(\frac{\Omega_f-\omega}{\Gamma}\right) + \arctan\left(\frac{\omega}{\Gamma}\right) - \frac{\pi}{2} \right], \tag{53}$$

where Ω_f is the transition frequency at the Fermi surface of the electrons and holes. It is related to the carrier density N by

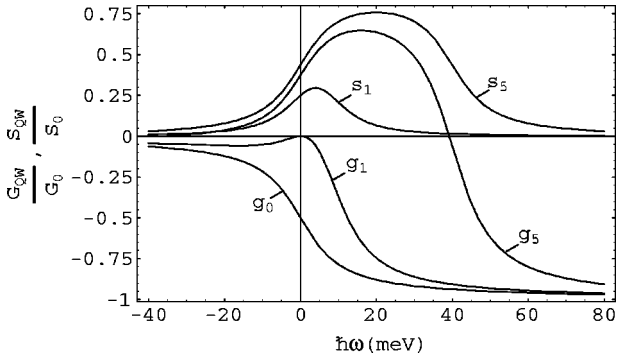

FIG. 3. Spectra of gain and spontaneous emission for a quantum well structure of $Q=5$ quantum wells given relative to $G_{max}=2.5\times10^7\ \mathrm{cm\,s^{-1}}\delta(r_z-z_0)$ and $S_{max}=2.7\times10^7\ \mathrm{cm^{-2}}$. The five spectra shown are the gain at $N=0$ (g_0), the gain at $N=10^{12}\ \mathrm{cm^{-2}}$ (g_1), the spontaneous emission at $N=10^{12}\ \mathrm{cm^{-2}}$ (s1), the gain at $N=5\times10^{12}\ \mathrm{cm^{-2}}$ $(g5)$ and the spontaneous emission at $N=5\times10^{12}\ \mathrm{cm^{-2}}$ (s5).

$$\Omega_f = \frac{\pi\hbar}{Q} \frac{m^e_{eff}+m^h_{eff}}{m^e_{eff} m^h_{eff}} N. \tag{54}$$

The spectral density of spontaneous emission is thus given by

$$S_{QW}(\omega) = \rho_{light} g_0^2 \frac{2Q\nu_0}{3\pi\hbar} \frac{m^e_{eff} m^h_{eff}}{m^e_{eff}+m^h_{eff}} \times \left[\arctan\left(\frac{\Omega_f-\omega}{\Gamma}\right) + \arctan\left(\frac{\omega}{\Gamma}\right) \right]. \tag{55}$$

Typical spectra of gain and spontaneous emission of an active layer containing $Q=5$ quantum wells obtained from the analytic approximations (53) and (55), respectively, are presented in Fig. 3 for characteristic values of the carrier density. For the spectra in Fig. 3 we have assumed a total spontaneous emission lifetime of $\tau_s=3$ ns and a band gap of $\hbar\omega_0=1.5$ eV. Other parameters are the effective mass of electrons $(m^e_{eff}=0.067m_0)$ and holes $(m^h_{eff}=0.053m_0)$, given in units of the electron mass m_0 as well as the dipole damping rate $\hbar\Gamma=8$ meV, and dielectric constant $\epsilon_r=12$. Gain and spontaneous emission are both displayed relative to the peak values $S_{max}=2.7\times10^7\ \mathrm{cm^{-2}}$ and $G_{max}=(2.5\times10^7\ \mathrm{cm\,s^{-1}})\delta(r_z-z_0)$. The gain value may be interpreted by calculating the gain of a light beam of width $\sigma^{-1}=10^{-5}$ cm with an incidence perpendicular with respect to the quantum well and traveling at a speed of $10^{10}\ \mathrm{cm\,s^{-1}}$ in the plane of the quantum well. The maximal gain is then given by $250\ \mathrm{cm^{-1}}$. The five spectra displayed in Fig. 3 are the gain at $N=0$ (g_0), the gain at $N=10^{12}\ \mathrm{cm^{-2}}$ (g_1), the spontaneous emission at $N=10^{12}\ \mathrm{cm^{-2}}$ (s_1), the gain at $N=5\times10^{12}\ \mathrm{cm^{-2}}$ (g_5) and the spontaneous emission at $N=5\times10^{12}\ \mathrm{cm^{-2}}$ (s_5). Figure 3 clearly shows the influence of the carrier density N. In the absence of charge carriers (g_0), the laser is purely absorptive. With increasing carrier density N, transparency is reached at $N=10^{12}\ \mathrm{cm^{-2}}$ (g_1). This density is characterized by vanishing gain (i.e., there is neither gain nor absorption) at a frequency of $\hbar\omega=0$. At the same time, however, there is a significant contribution of

spontaneous emission (s_1) with a maximum at a frequency of $\hbar\omega \approx 4$ meV. Finally, at high values of the carrier density ($N = 5\times 10^{12}$ cm^{-2}), both gain (g_5) and spontaneous emission (s_5) have a maximum above the band-gap frequency.

B. Spontaneous emission factor and far-field pattern of an edge emitting laser

In the optical cavity of a laser the equations for gain and spontaneous emission are modified by the mode structure. In particular, the total linear response of an electromagnetic field mode inside the cavity includes the cavity loss rate κ. For the edge emitting semiconductor laser, the gain function of the cavity modes is given by

$$G_{1D}(\omega) = g_0^2 \frac{\nu_0}{4\pi^2}\sigma \int d^2\mathbf{k}_\parallel \frac{\Gamma(\mathbf{k}_\parallel)+\kappa}{(\Gamma(\mathbf{k}_\parallel)+\kappa)^2+(\Omega(\mathbf{k}_\parallel)-\omega)^2} \times [f^e(k_\parallel)+f^h(k_\parallel)-1], \tag{56}$$

where the confinement factor σ is defined according to Eq. (37). Spontaneous emission into the cavity modes passes through the gain medium and is thereby absorbed or amplified accordingly. Thus for an edge emitting laser, the rate of spontaneous emission into a cavity mode of frequency ω is given by

$$S_{1D}(\omega) = 2g_0^2 \frac{\nu_0}{4\pi^2}\sigma \int d^2\mathbf{k}_\parallel \times \frac{\Gamma(\mathbf{k}_\parallel)+\kappa}{[\Gamma(\mathbf{k}_\parallel)+\kappa]^2+[\Omega(\mathbf{k}_\parallel)-\omega]^2} f^e(k_\parallel) f^h(k_\parallel). \tag{57}$$

This rate represents the total rate of spontaneous emission events per mode, regardless of the actual width of the laser. On the other hand, Eq. (50) gives the total rate of spontaneous emission per quantum well area.

1. Spontaneous emission factor

In a laser of length L and total width W (c.f. Fig. 1), the spontaneous emission rate into free space is $LW\,S_{total}$. The spontaneous emission factor β, which is generally defined as the fraction of spontaneous emission being emitted into the cavity mode [2], is on the basis of our theory given by the expression

$$\beta(\omega, N_{1D}) = \frac{\tau_s S_{1D}}{W N_{1D}}. \tag{58}$$

Note that the two-dimensional carrier density N in the quantum well is related to the one-dimensional carrier density N_{1D} by $N_{1D} = LN$. The spontaneous emission factor β is a function of both frequency and carrier density. Consequently, the common assumption of the spontaneous emission factor β being independent of the carrier density [2,7] may be regarded as an approximation similar to the assumption of linear gain.

An analytical expression for the spontaneous emission factor may be obtained for zero temperature. The k-space integrals may then be solved analytically using Eq. (20) and assuming that Γ is independent of $\mathbf{k}_\parallel$. For the spontaneous emission factor β, the analytical result reads

$$\beta(\omega, \Omega_f) = \frac{3\sigma}{2\pi\rho_{light} QWL\Omega_f} \times \left[\arctan\left(\frac{\Omega_f-\omega}{\Gamma+\kappa}\right) + \arctan\left(\frac{\omega}{\Gamma+\kappa}\right)\right]. \tag{59}$$

The Fermi frequency Ω_f is defined by Eq. (54) and expresses, in particular, the carrier density dependence of β. For $\Omega_f, \omega \ll \Gamma+\kappa$ we recover the result typically given in the literature (e.g., [2]), which does not depend on N. Figure 4 shows the deviation of the spontaneous emission factor from this value as the Fermi frequency Ω_f passes the point of resonance with the cavity mode. Figure 4 illustrates, in particular, the carrier density dependence of β for three modes with frequencies above the band-gap frequency given by (a) $\omega = 0$, (b) $\omega = 0.5(\Gamma+\kappa)$, and (c) $\omega = \Gamma+\kappa$. Most notably, β is always smaller than the usual estimate given by $\beta(\omega = \Omega_f = 0)$, which is based on the assumption of ideal resonance between the transition frequency and the cavity mode.

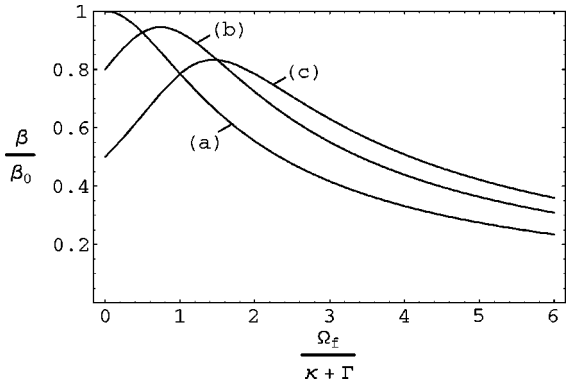

FIG. 4. Carrier density dependence of the spontaneous emission factor β for three modes with frequencies above the band-gap frequency given by (a) $\omega = 0$, (b) $\omega = 0.5(\Gamma+\kappa)$, and (c) $\omega = \Gamma+\kappa$. $\beta_0 = \beta(\omega = N = 0)$ is determined by the geometry of the laser. The carrier density is given in terms of the transition frequency at the Fermi edge Ω_f.

2. Far-field pattern of a broad area laser

With Eqs. (56) and (57), it is possible to find the steady state intensity I_s of a mode with frequency ω,

$$I_s(\omega) = \frac{S_{1D}(\omega)}{2\kappa - 2G_{1D}(\omega)}. \tag{60}$$

Note that this result may also be obtained directly from Eqs. (36a–36e). In a wide cavity, the cavity modes are approximately plane wave modes and the relation between $I_0(\omega)$ and $I_0(r_x; r_x')$ in that case reads

$$I_0(r_x, r_x') = \int dq e^{iq(r_x - r_x')} I\left(\omega = \frac{\omega_0 q^2}{2k_0^2 \epsilon_r}\right). \tag{61}$$

The steady state intensity distribution is characterized by the spatial coherence derived from the intensity distribution of

the plane wave modes of the cavity. Generally, the intensity distribution of plane waves corresponds in the far-field to an optical field at angles relative to the axis of emission in the plane of the quantum well. The angular distribution of intensity and coherence in the far field is thus given by

$$I_f(\Theta,\Theta')=\frac{k_0}{2\pi}\int dr_x dr_x' e^{ik_0\Theta r_x} I_0(r_x,r_x') e^{-ik_0\Theta' r_x'}. \tag{62}$$

Therefore, the far field intensity distribution may be determined directly from the frequency dependence of the intensities by

$$I_f(\Theta,\Theta)=Wk_0 I_s\left(\omega=\frac{\omega_0\Theta^2}{2\epsilon_r}\right), \tag{63}$$

the intensity is given in units of $2\kappa\hbar\omega_0$ per unit angle.

For $T=0$ we may in analogy to Eq. (59) solve the integral in Eq. (57) by assuming Γ to be independent of $\mathbf{k}$. As an analytical expression we then obtain for the far-field intensity distribution of a broad area semiconductor laser

$$I_f(\Theta,\Theta) = Wk_0 \frac{\arctan\left(\frac{\Omega_f-\omega(\Theta)}{\Gamma+\kappa}\right)+\arctan\left(\frac{\omega(\Theta)}{\Gamma+\kappa}\right)}{\pi\left(R+\frac{1}{2}\right)-2\arctan\left(\frac{\Omega_f-\omega(\Theta)}{\Gamma+\kappa}\right)-\arctan\left(\frac{\omega(\Theta)}{\Gamma+\kappa}\right)},$$

$$\text{with } R=\frac{2\hbar\kappa}{g_0^2\nu_0\sigma}\frac{m_{eff}^e+m_{eff}^h}{m_{eff}^e m_{eff}^h} \text{ and } \omega(\Theta)=\frac{\omega_0\Theta^2}{2\epsilon_r}. \tag{64}$$

The parameter R represents the ratio between the cavity loss rate κ and the maximum amplification rate of the gain medium. Laser activity is only possible if $R<1$. The classical laser threshold is defined by the carrier density for which the denominator of $I_f(\Theta,\Theta)$ is zero for a single specific frequency $\omega(\Theta)$. Consequently, the carrier density at which this occurs is pinned. Figure 5 shows the far field intensity distribution for different carrier densities below this pinning density. In Fig. 5(a), the wide intensity distribution of amplified spontaneous emission for carrier densities is much lower than the pinning density. The intensity maximum is clearly located at $\Theta=0$. Figure 5(a) shows the intensity distribution for carrier densities halfway towards threshold. Already, the intensity maxima move to angles of $\pm 15°$, corresponding to the frequency at which the gain spectrum has its maximum. In the case of Fig. 5(c), the threshold region is very close to the pinning density. The peaks in the far-field pattern narrow as the laser intensity is increased. Consequently the far-field pattern indeed is a measure of the spatial coherence—similar as the linewidth of the laser spectrum is a measure of temporal coherence. It is therefore desirable to consider quantum noise effects in the spatial patterns of optical systems. In the context of squeezing, such patterns have been investigated by Gatti and co-workers [26] based on the general formulation of Lugiato and Castelli [27]. The laser patterns presented here are based on the same principles. Usually, however, the strong dissipation prevents squeezing in laser systems unless the pump-noise fluctuations are suppressed [28].

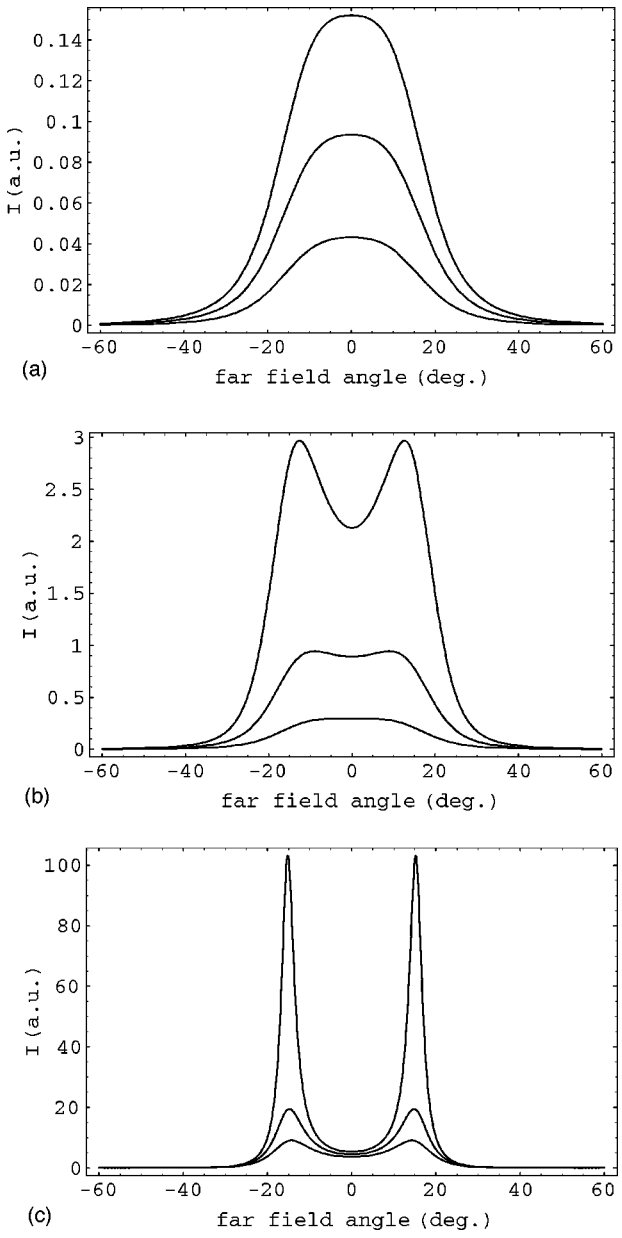

FIG. 5. Far-field intensity distributions for $R=0.5$, $\hbar\omega_0=1.5$ eV, $\hbar(\Gamma+\kappa)=8$ meV, and $\epsilon_r=12$. The density is pinned at $\Omega_f=1.8805(\Gamma+\kappa)$. (a) shows the far-field pattern for carrier densities of 0.05, 0.10, and 0.15 times pinning density, (b) shows the distribution for 0.25, 0.5, and 0.75 times pinning density and (c) shows the distribution for 0.90, 0.95, and 0.99 times the pinning density. The peaks appear at emission angles of $\pm 15°$.

VII. CONCLUSIONS

The quantum Maxwell-Bloch equations (QMBE) for spatially inhomogeneous semiconductor lasers derived in this paper take into account the quantum mechanical nature of the light field as well as that of the carrier system. The only approximation used in the derivation of the intensity and correlation dynamics is that of statistical independence be-

tween the two carrier systems and the light field. In the QMBE presented here, the effects of coherent spatiotemporal quantum fluctuations, which are generally not considered in the semiclassical Maxwell-Bloch equations for semiconductor laser devices have thus been taken into account.

The spontaneous emission term appears side by side with the gain and absorption term in the dynamics of the field-dipole correlation. In this way the spatial coherence of spontaneous emission and amplified spontaneous emission is consistently described by the quantum Maxwell-Bloch equations. Typical features of the model have been illustrated by the spectra of gain and spontaneous emission. An example of the spatial coherence characteristics described by the quantum Maxwell-Bloch equations has been presented by analytically obtaining the spontaneous emission factor β and the far-field distribution for the example of a broad area edge emitting laser. In general the quantum Maxwell-Bloch equations derived for edge emitting and vertical cavity surface emitting lasers provide a starting point for a detailed analysis of spatial coherence patterns in diverse semiconductor laser geometries such as broad area or ultralow threshold lasers.

[1] O. Hess and T. Kuhn, Prog. Quantum Electron. **20**, 85 (1996).
[2] K.J. Ebeling, *Integrated Optoelectronics* (Springer, Berlin, 1993).
[3] T. Lee, C.A. Burrus, J.A. Copeland, A.G. Dentai, and D. Marcuse, IEEE J. Quantum Electron. **QE-18**, 1101 (1982).
[4] K. Petermann, IEEE J. Quantum Electron. **QE-15**, 566 (1979).
[5] A. Yariv and S. Margalit, IEEE J. Quantum Electron. **QE-18**, 1831 (1982).
[6] A.E. Siegmann in *Coherence and Quantum Optics VII*, edited by J. Eberly, L. Mandel, and E. Wolf (Plenum, New York, 1996).
[7] G. Björk, A. Karlsson, and Y. Yamamoto, Phys. Rev. A **50**, 1675 (1994).
[8] Y. Yamamoto and R.E. Slusher, Phys. Today **46** (6), 66 (1993).
[9] F. Jahnke, K. Henneberger, W. Schäfer, and S.W. Koch, J. Opt. Soc. Am. B **10**, 2394 (1993).
[10] F. Jahnke and S.W. Koch, Phys. Rev. A **52**, 1712 (1995).
[11] K. Henneberger and S.W. Koch, Phys. Rev. Lett. **76**, 1820 (1996).
[12] O. Hess and T. Kuhn, Phys. Rev. A **54**, 3347 (1996).
[13] P.Y. Yu and M. Cardona, *Fundamentals of Semiconductors* (Springer, Berlin, 1996).
[14] E. Wigner, Phys. Rev. **40**, 749 (1932).
[15] M. San Miguel, Q. Feng, and J.V. Moloney, Phys. Rev. A **52**, 1728 (1995).
[16] J. Martin-Regalado, M. San Miguel, N.B. Abraham, and F. Prati, Opt. Lett. **21**, 351 (1995).
[17] H.F. Hofmann and O. Hess, Phys. Rev. A **56**, 868 (1997).
[18] H. van der Lem and D. Lenstra, Opt. Lett. **22**, 1698 (1997).
[19] H.F. Hofmann and O. Hess, Quantum Semiclassic. Opt. **10**, 87 (1998).
[20] A.K.J. van Doorn, M.P. van Exter, A.M. van der Lee, and J.P. Woerdman, Phys. Rev. A **55**, 1473 (1997).
[21] W.W. Chow, S.W. Koch, and M. Sargent, *Semiconductor-Laser Physics* (Springer, Berlin, 1994).
[22] T. Kuhn and F. Rossi, Phys. Rev. Lett. **69**, 977 (1992); **46**, 7496 (1992).
[23] C. Ell, R. Blank, S. Benner, and H. Haug, J. Opt. Soc. Am. B **6**, 2006 (1989).
[24] H.F. Hofmann and O. Hess, Opt. Lett. **23**, 391 (1998).
[25] D.F. Walls and G.J. Milburn, *Quantum Optics* (Springer, Berlin, 1994).
[26] A. Gatti, H. Wiedemann, L.A. Lugiato, I. Marzoli, G. Oppo, and S.M. Barnett, Phys. Rev. A **56**, 877 (1997).
[27] L.Q. Lugiato and F. Castelli, Phys. Rev. Lett. **68**, 3284 (1992).
[28] Y. Yamamoto, S. Machida, and O. Nilsson, Phys. Rev. A **34**, 4025 (1986).